Dilatometry Simulation of Continuous Annealing/Galvanizing Thermal Cycle Effects on AHSS Microstructure and Properties

Case I: Fives Keods DP1000
Second progress report

Project Overview

IZA Program "ZCO-69 Galvanizing Thermal Cycle Effects on AHSS Properties"

NORTH AMERICAN GAP PROGRAM REVIEW MEETING
October 21-22, 2015 TOLEDO, OHIO, USA

Objective: To determine the influence of galvanizing/galvannealing or annealing/overaging thermal cycles on microstructure and mechanical properties.

Second progress report

- ☑JMatPro determination of volume fractions of individual phases as a function of temperature.
- ☑Dilatometry simulation of thermal cycles on tension test sub-size specimen.
- ☑Evaluation of the mechanical properties (yield strength, tensile strength, elongation and harness).
- ☑Identification and quantification of micro-constituent volume fractions by the SEM/EBSD technique.
- ☑Microstructure and mechanical properties for additional cooling rates (1 and 100 °C/s).

Chemical composition of DP1000 Steel (wt%)

Steel*	C	Mn	P	S	N	Si	Cu	Ni	Cr	Nb	Mo	Ti	V
DP1000	0.18	1.79	0.024	0.002	0.0006	0.333	0.076	0.050	0.43	0.030	0.01	0.026	0.004

*Resulting of optical spectrometry analysis and LECO

Microstructure and mechanical properties

Steel	YS (MPa)	UTS (MPa)	EL (%)	*HRC*
DP1000	974	1038 ± 5	5.5 ± 0.4	25 ±2.47

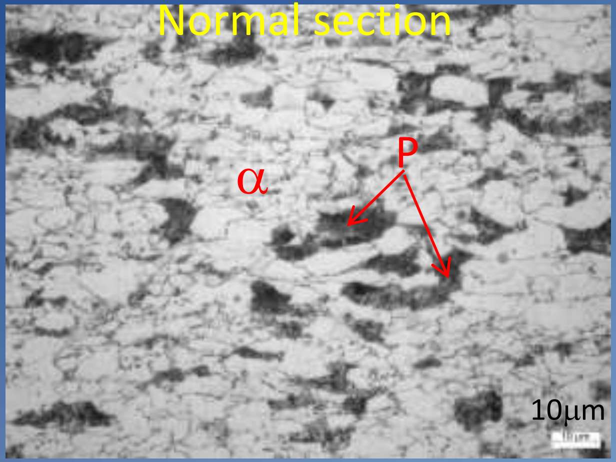

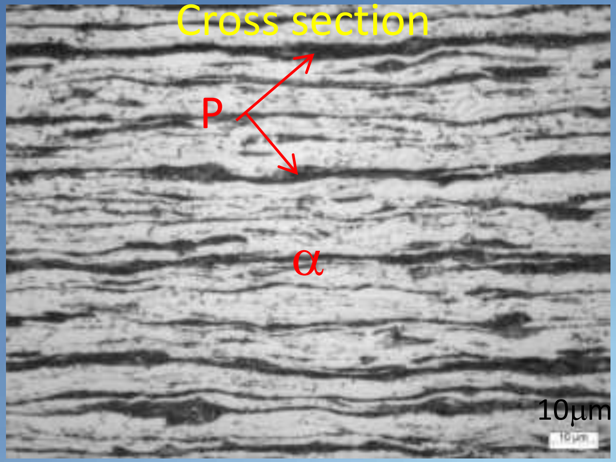

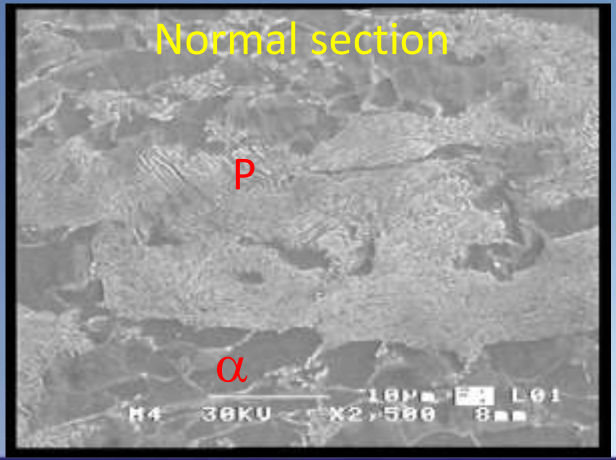

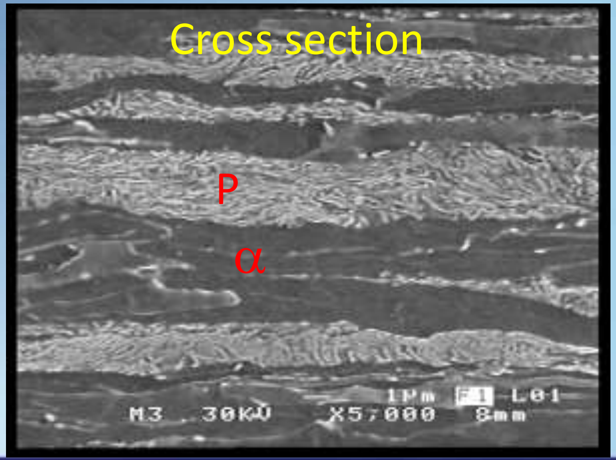

Critical transformation temperatures

Critical temperatures (Ac_1, Ac_3, M_s y M_f) determined from austenitizing at 1000°C for 5 min followed of quenching with helium gas.

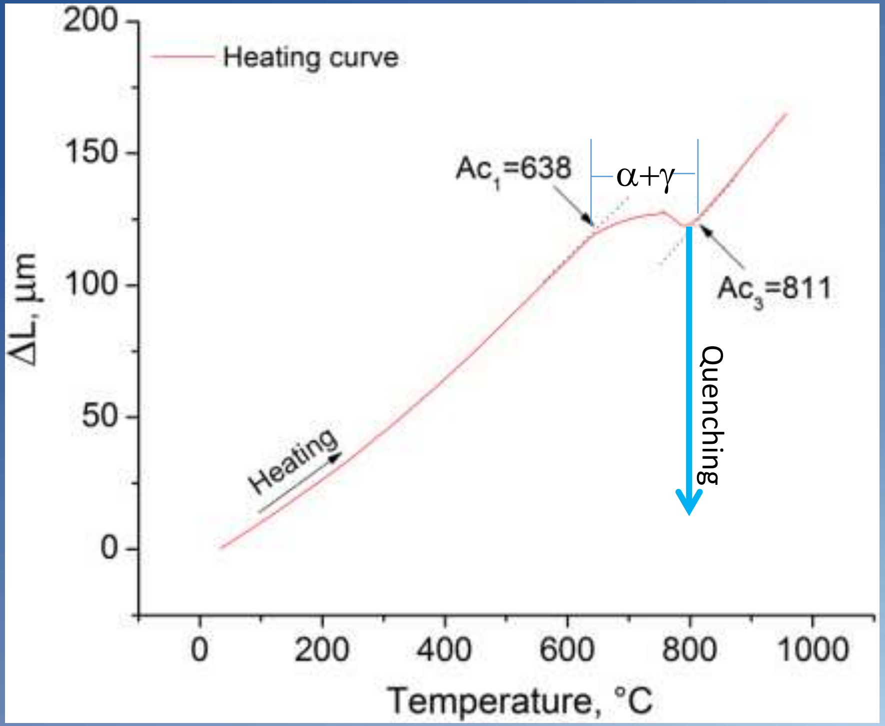

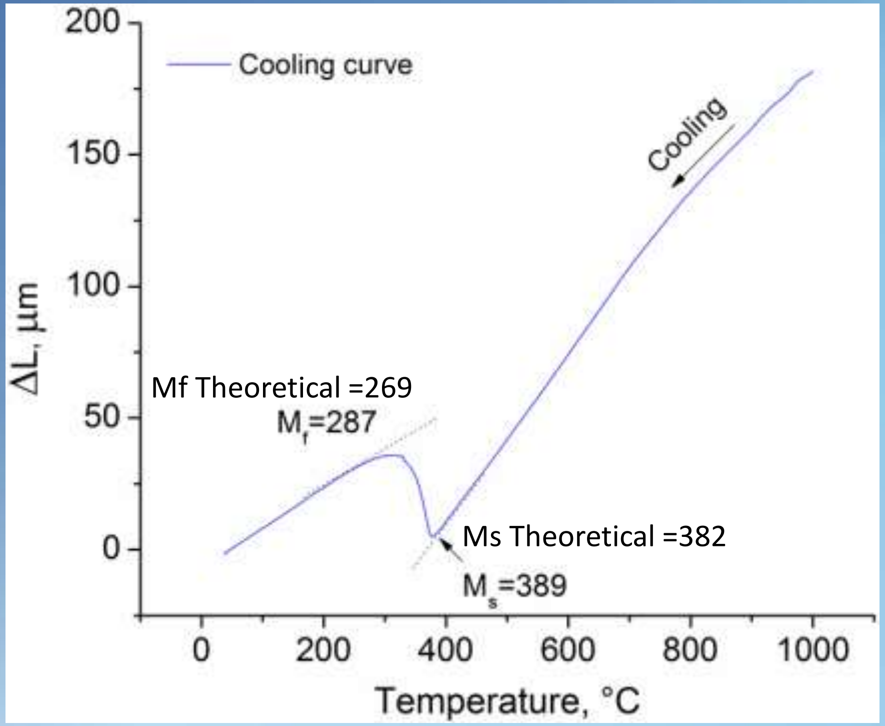

Tension test

E 8M – 04

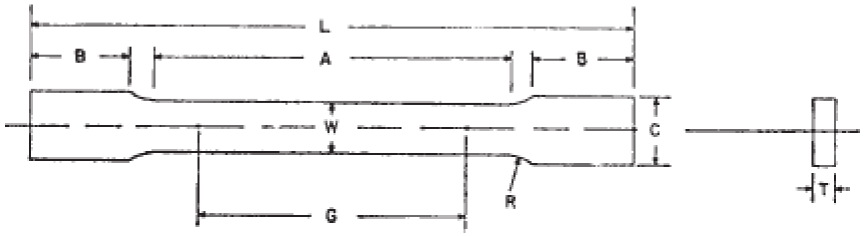

Dimensions, mm			
	Standard Specimens		Subsize Specimen
Nominal Width	Plate-Type 40 mm	Sheet-Type 12.5 mm	6 mm
G— Gage length (Note 1 and Note 2)	200.0 ± 0.2	50.0 ± 0.1	25.0 ± 0.1
W— Width (Note 3 and Note 4)	40.0 ± 2.0	12.5 ± 0.2	6.0 ± 0.1
T— Thickness (Note 5)		thickness of material	
R— Radius of fillet, min (Note 6)	25	12.5	6
L— Overall length, (Note 2, Note 7 and Note 8)	450	200	100
A— Length of reduced section, min	225	57	32
B— Length of grip section, (Note 8)	75	50	30
C— Width of grip section, approximate (Note 4 and Note 9)	50	20	10

Rectangular Tension Test Specimens

- **The tension test subsize specimens used in this research work were 0.25 the standard specimen.**

ASTM E8 Standard, Standard test methods for tension testing of metallic materials, 2011, ASTM International, West Conshohocken, PA, 2011, DOI: 10.1520/E0008_E0008M-11 www.astm.org. (2011), p. 27.

It is generally recognized that in order to compare elongation measurements of different-sized specimens, the specimen must be geometrically similar. The critical geometrical factor for which similitude must be maintened is $L_o/\sqrt{A_o}$ for sheet specimens or L_o/D_o for round bars. Different values of $L_o/\sqrt{A_o}$ are specified by the standardizing agencies in different countries. The following table gives some appropriate values.

Type Specimen	USA ASTM	Great Britain Before 196	Great Britain Current	Germany
Shett $L_o/\sqrt{A_o}$	4.5	4.0	5.65	11.3
Round L_o/D_o	4.0	3.54	5.0	10.0

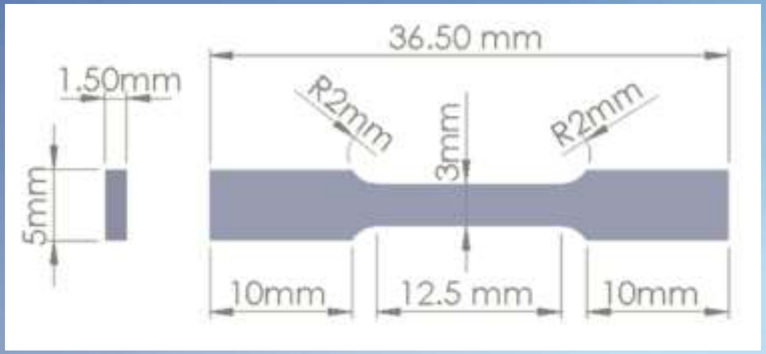

$L_o = 12.5$
$A = 1.5 \, x \, 3 = 4.5$
$\therefore L_o/\sqrt{A_o} = 5.8$

Critical geometrical factor for the designed subsize specimens.

Mechanical Metallurgy 3rd Edition, George E. Dieter.

In tensile testing using sub-size specimems is not possible to use an extensometer to measure strain. Therefore, the strain was estimated from the displacement of the machine cross-head during the test. For this case, the curve was adjusted as follows:

$$X_{Total} = X_{specimen} + X_{machine}$$

$$X_{specimen} = X_{Total} - X_{machine}$$

$$X_{machine} = \frac{F}{m}$$

Where *m* is the slope of the graph *F*- $\Delta L_{machine}$

$\therefore$ elongation$= \frac{\Delta L_{specimen}}{L_o}$

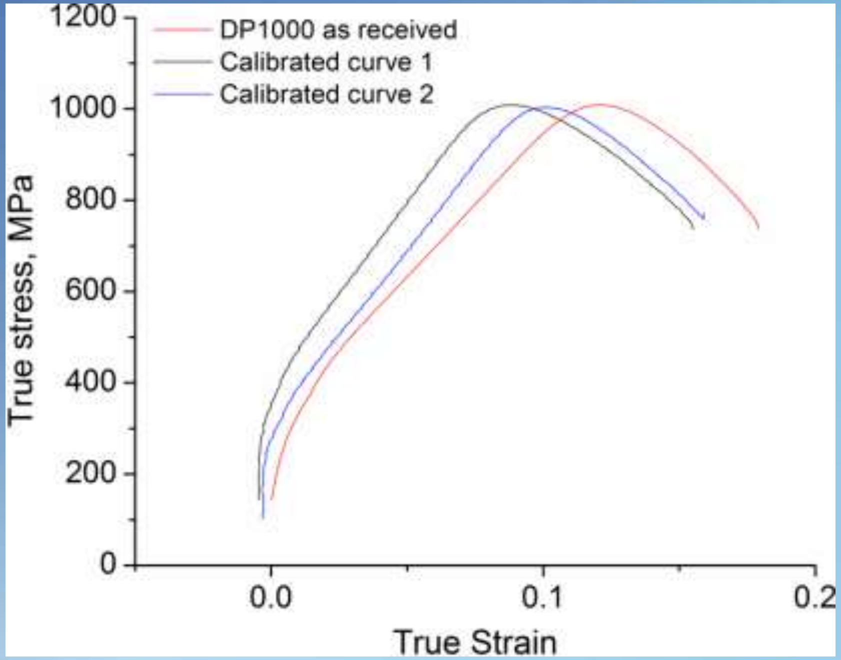

True stress-true strain curves resulting from tension test for DP1000 steel in as received condition.

Mechanical Metallurgy 3rd Edition, George E. Dieter.

Simulation of thermal cycles on tension test sub-size specimens.

In order to find the optimal size were carried out a lot of tension tests on specimens of different sizes.

Dilatometric curves resulting from Cycle A

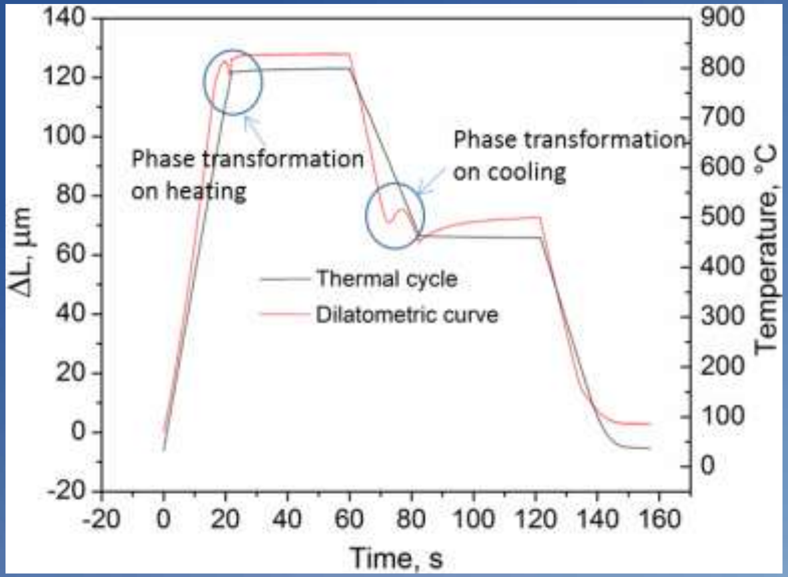

Simulation on standard flat specimen of 5 mm in width and 10 mm in length

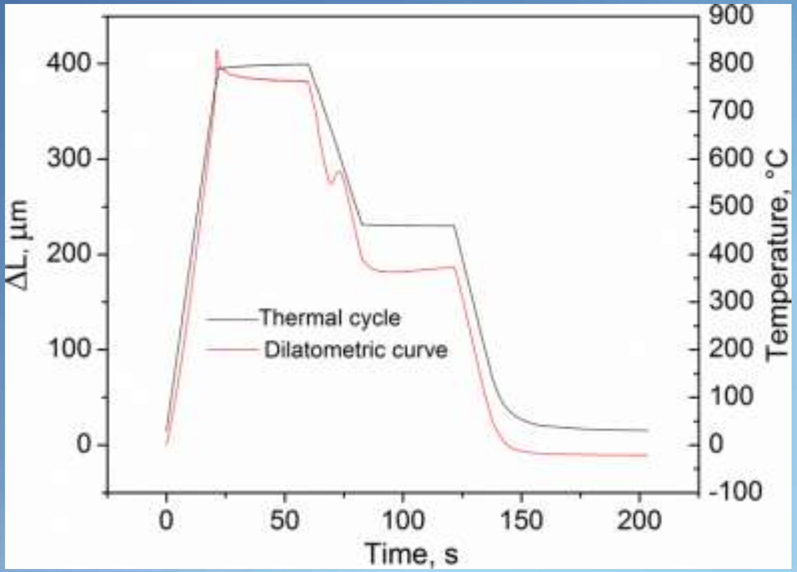

Simulation on tension test sub-size specimen

Microstructural characterization by OIM/EBSD

Orientation and image quality maps indicate the presence of at least three different phases

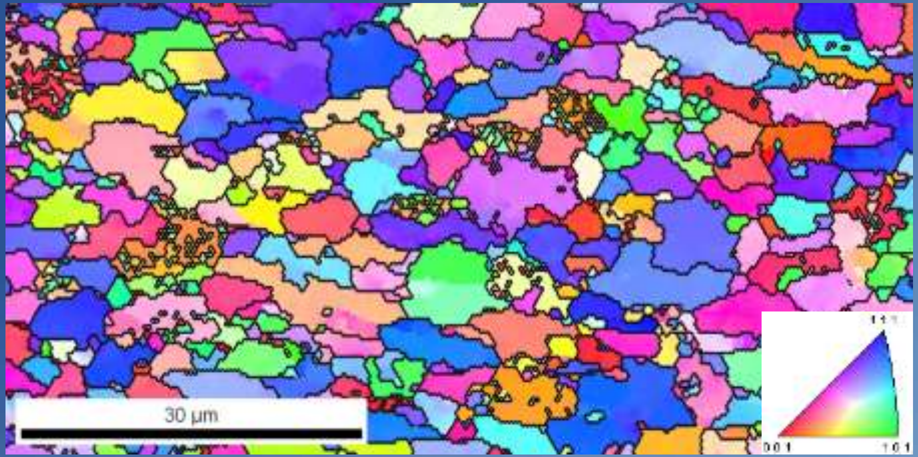

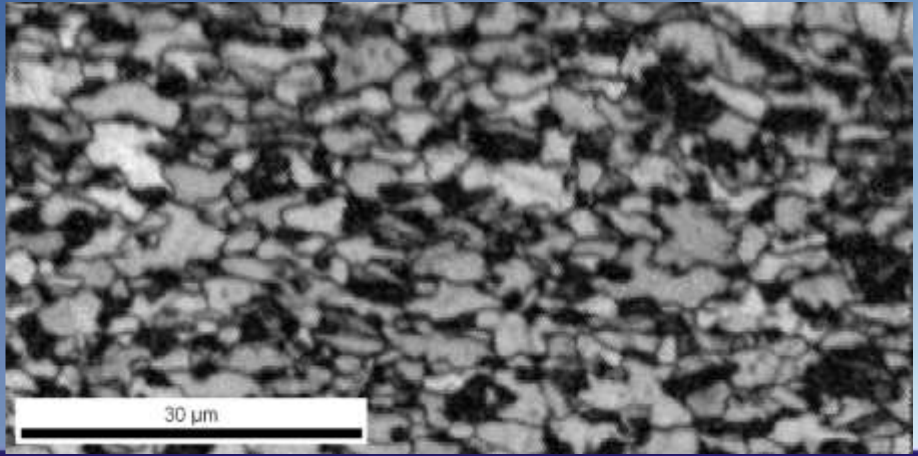

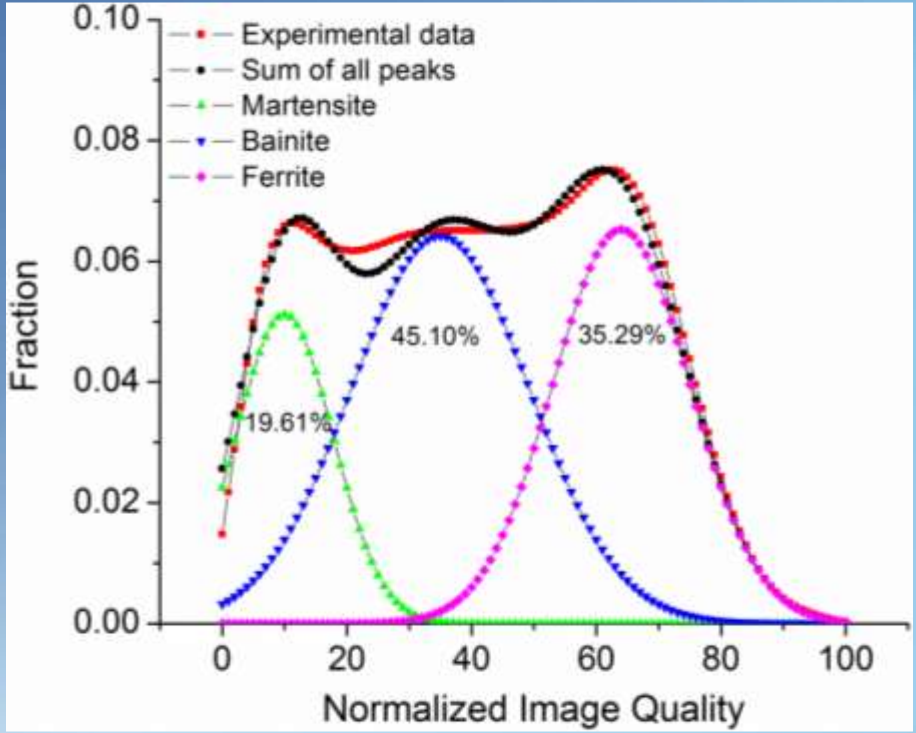

Simulation of continuous annealing and galvanizing thermal cycles

- Cycle A (Reference termal cycle for the customer)

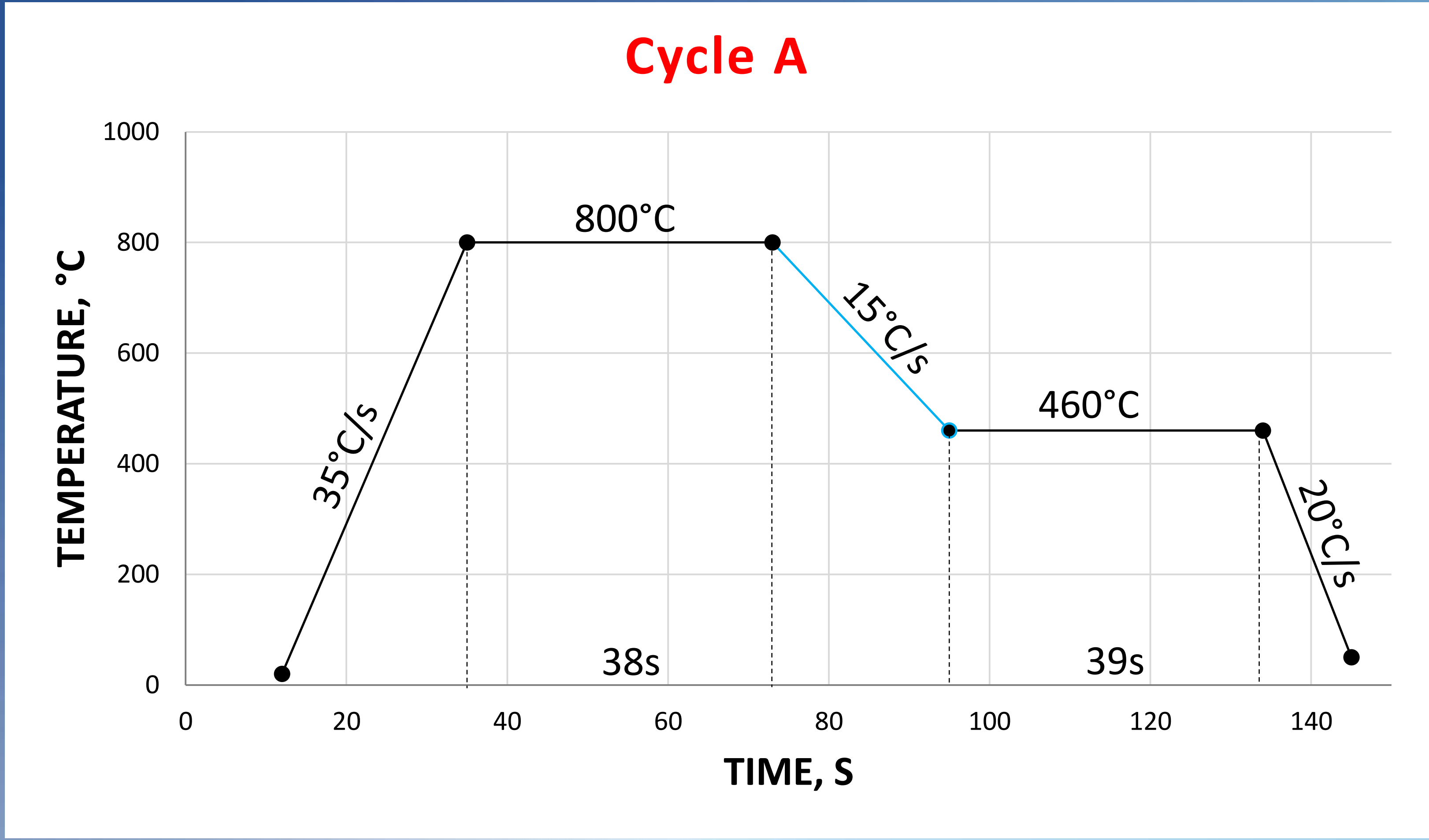

Theoretical phase transformations

Prediction of resulting phases according to the Cycle A. For this thermal cycle condition, the resulting microstructure would be a mixture of ferrite (α) and bainite (B).

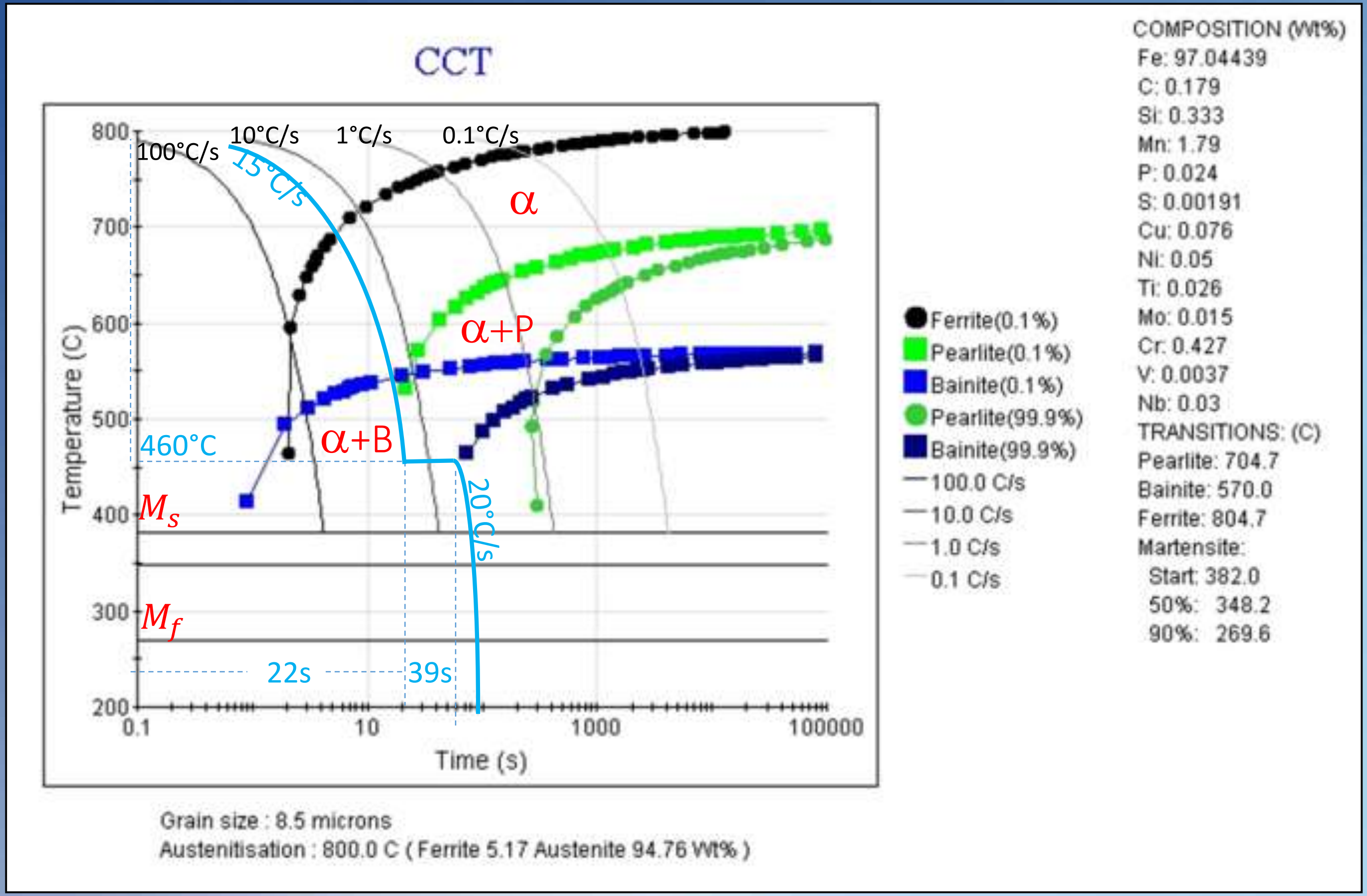

JMatPro calculation of linear contraction behavior as a function of temperature on cooling according to the thermal Cycle A.

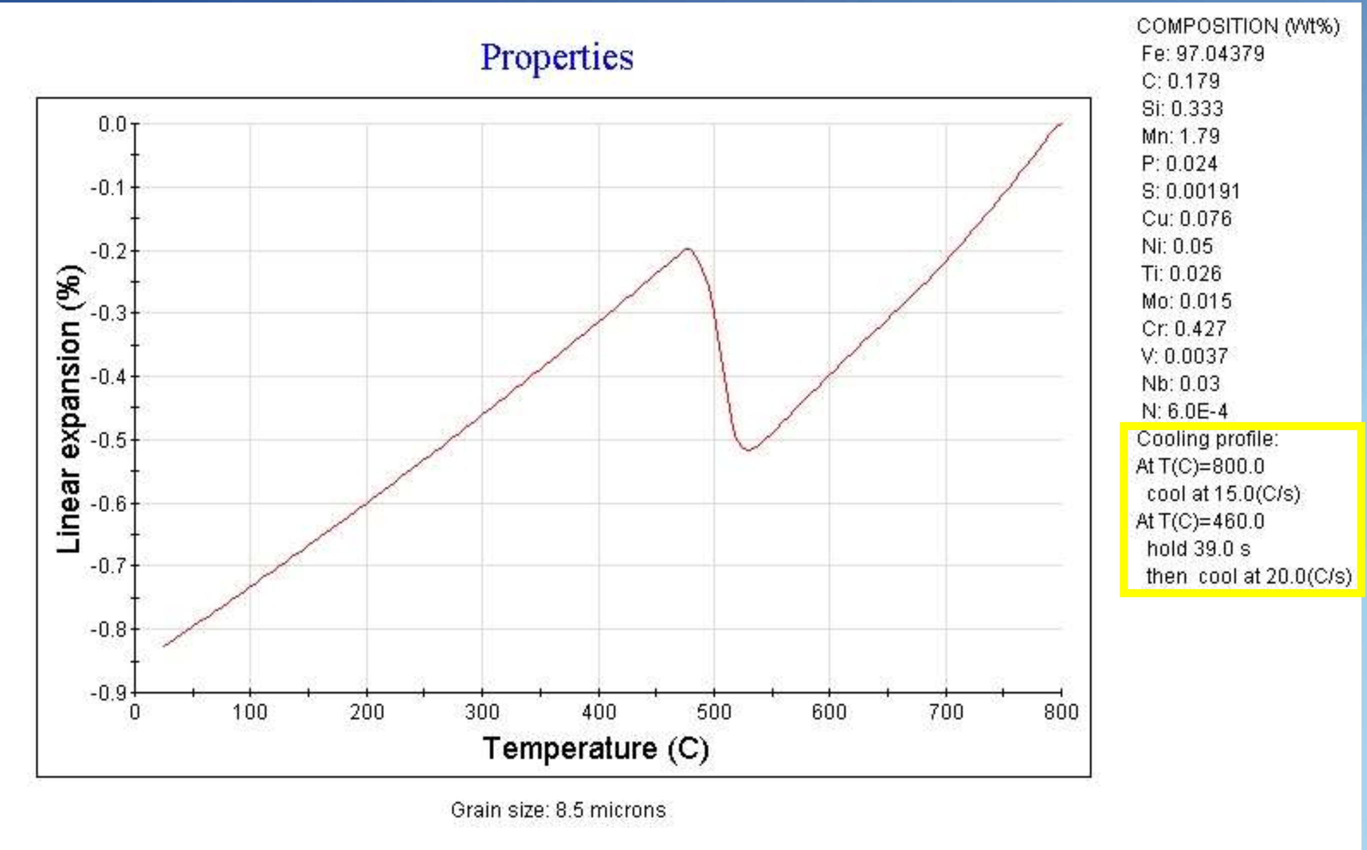

JMatPro calculation of temperature evolution of volume fractions of individual phases on cooling according to Cycle A. 78% bainite and 22% ferrite.

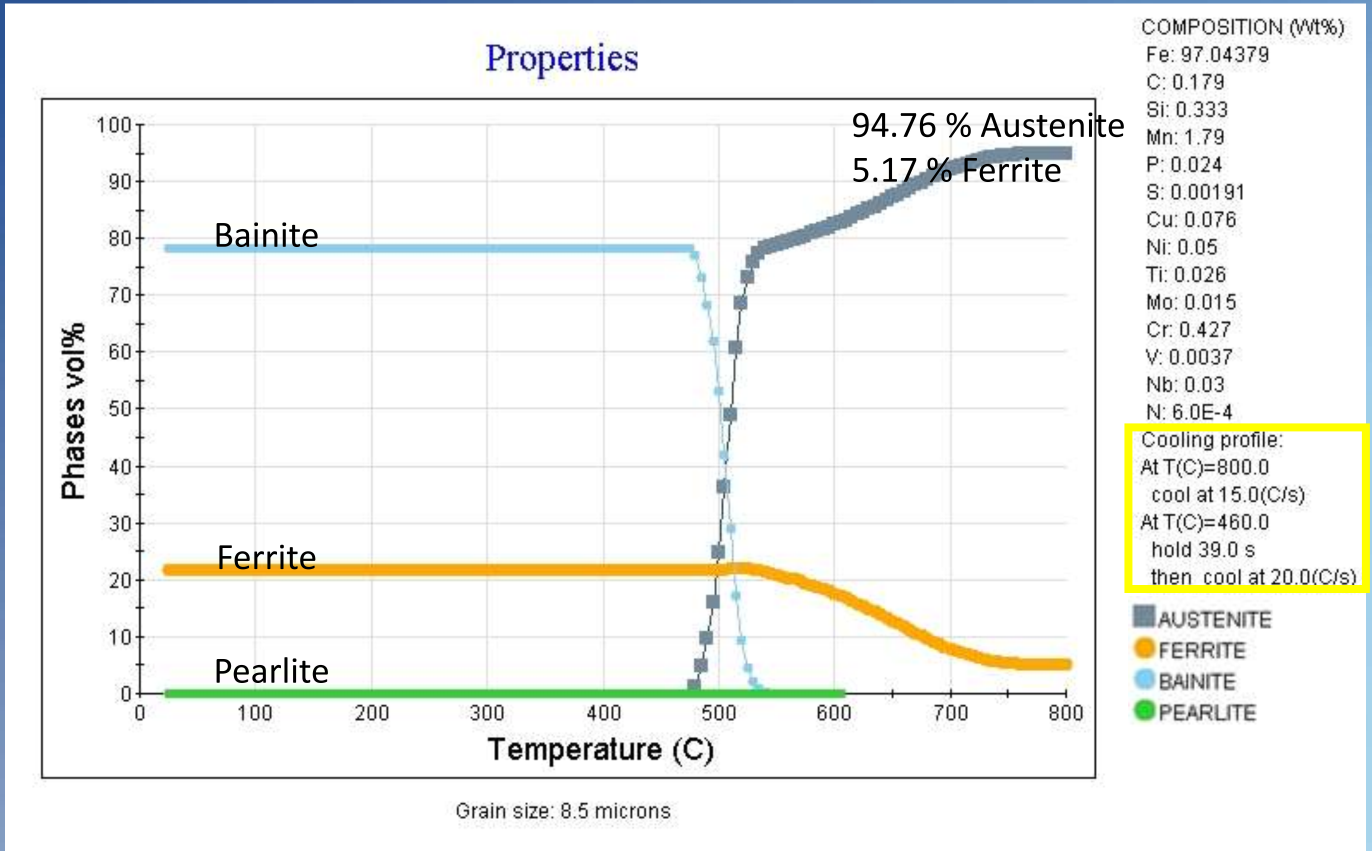

Dilatometry test

Dilatometric curves resulting from Cycle A for a standard flat specimen of 5 mm in width and 10 mm in length, machined from the as cold-rolled condition steels.

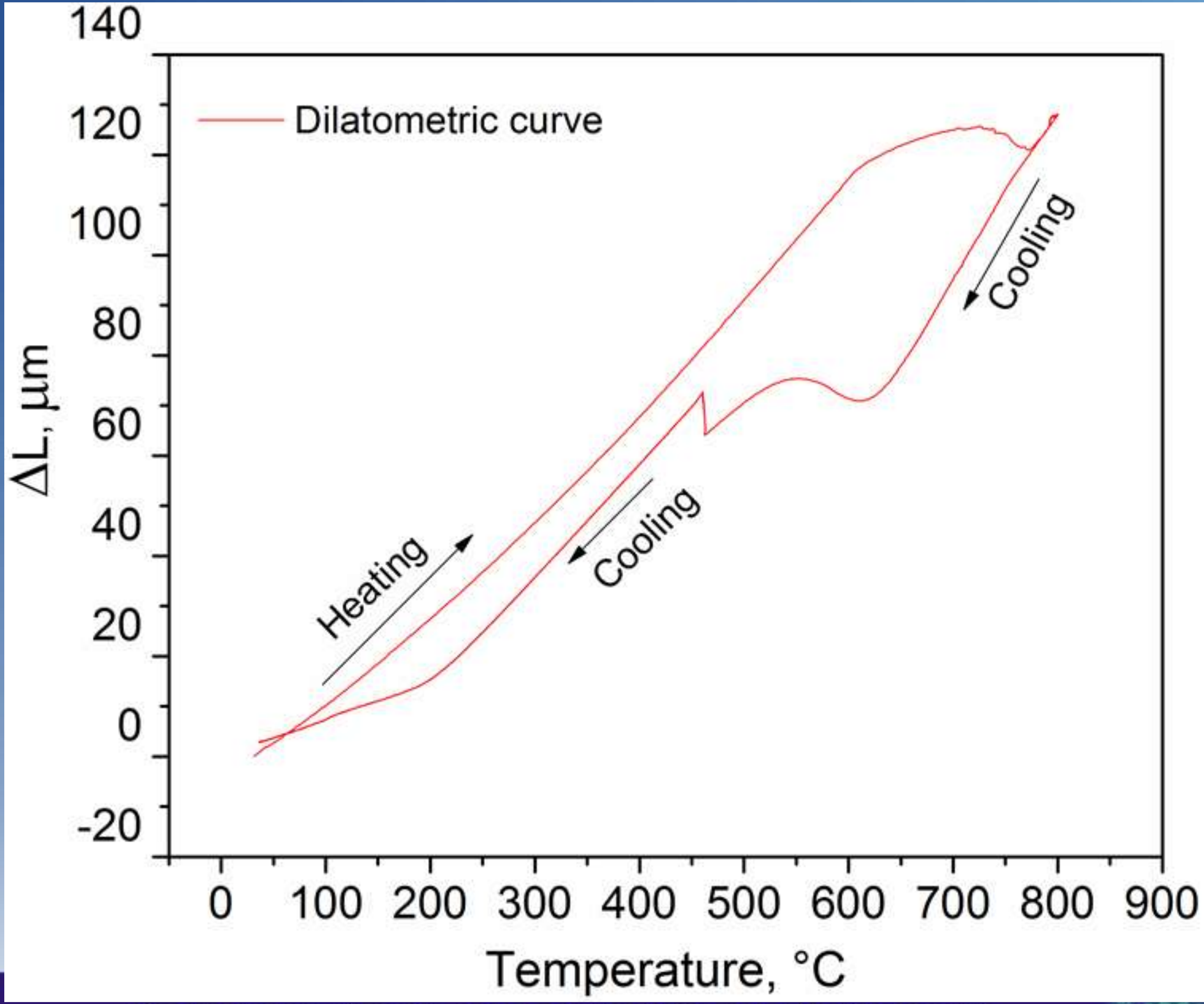

Metallographic characterization and hardness

Microstructures and hardness profile resulting of sample subjected to Cycle A.
The heat treated samples were etched with 2% nital

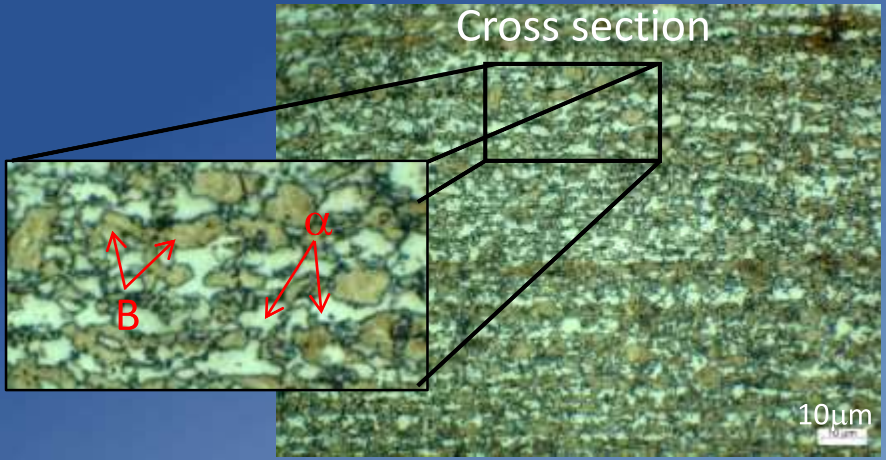

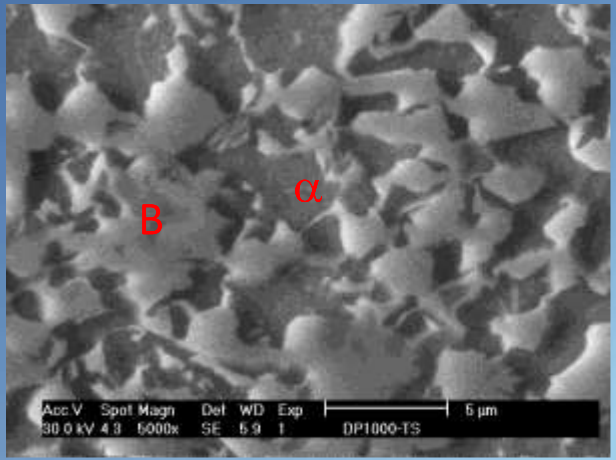

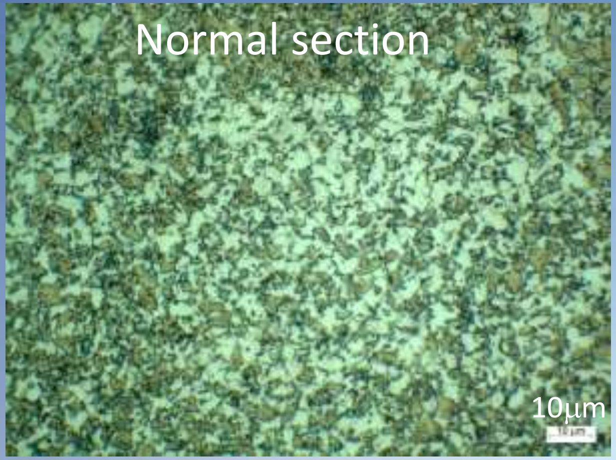

Tensile Sample
(Gauge Length)

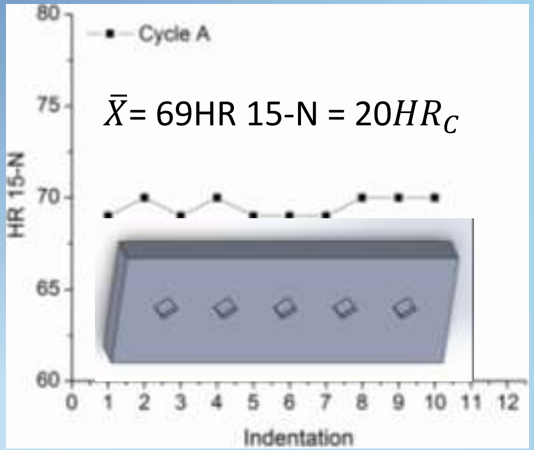

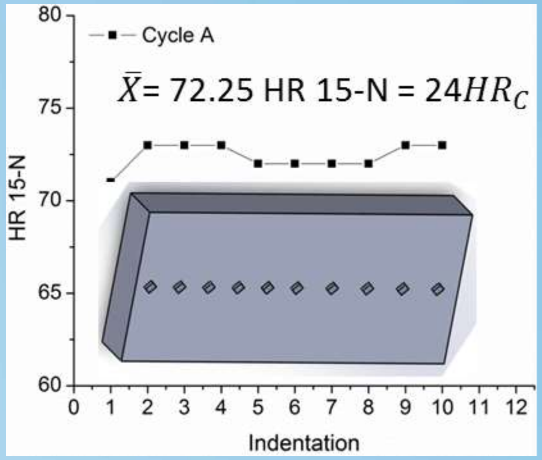

Microstructures resulting of sample subjected to Cycle A. The heat treated samples were etched with LePera.

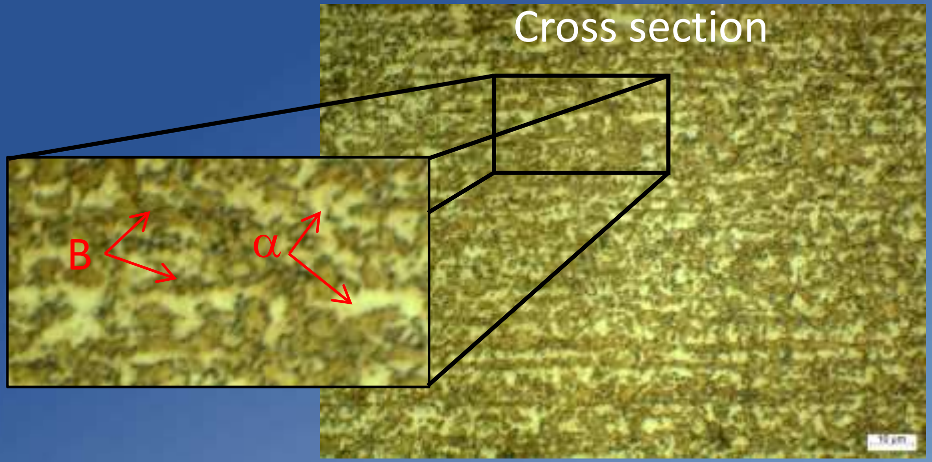

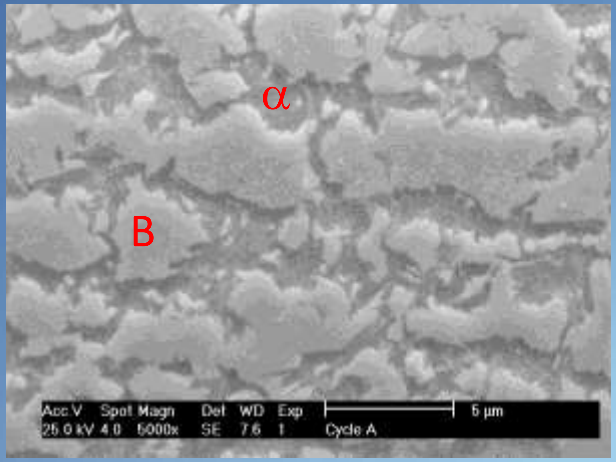

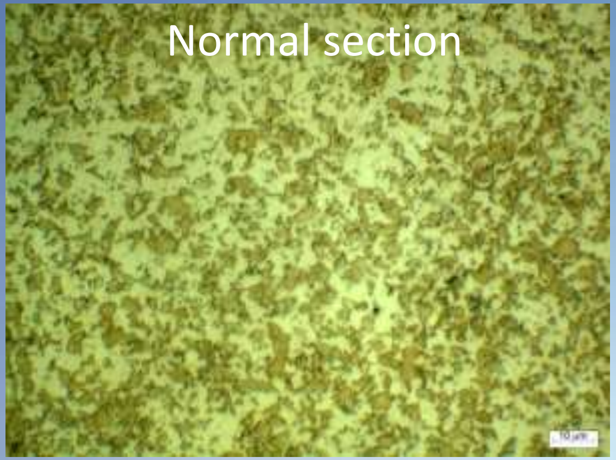

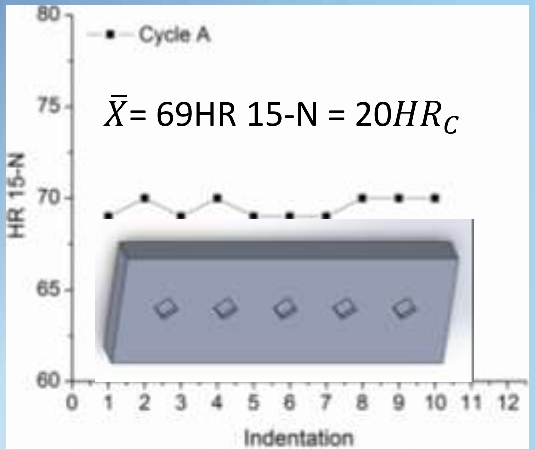

Microstructural characterization by OIM/EBSD

According to the processing of image quality values (IQ), the resulting phases from Cycle A are 19.61% martensite, 45.10% bainite and 35.29% ferrite.

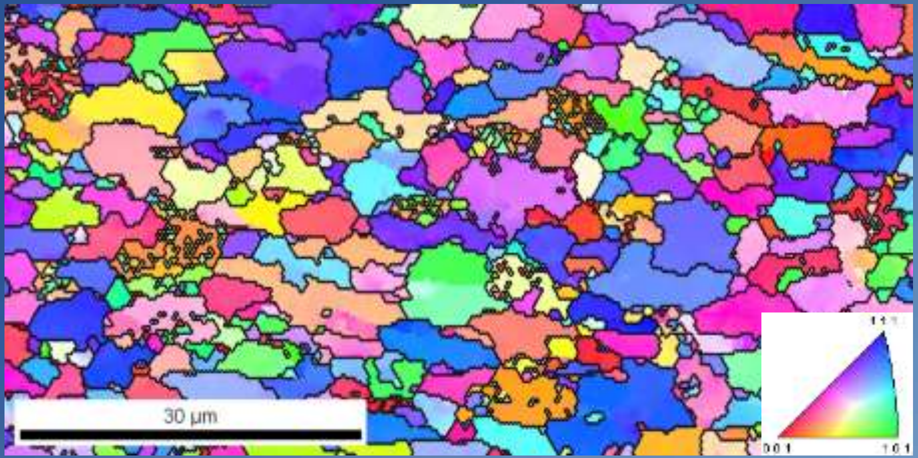

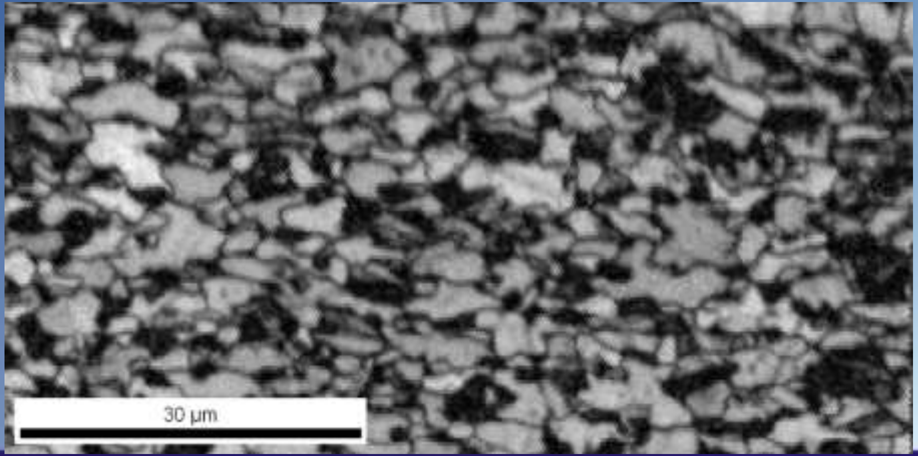

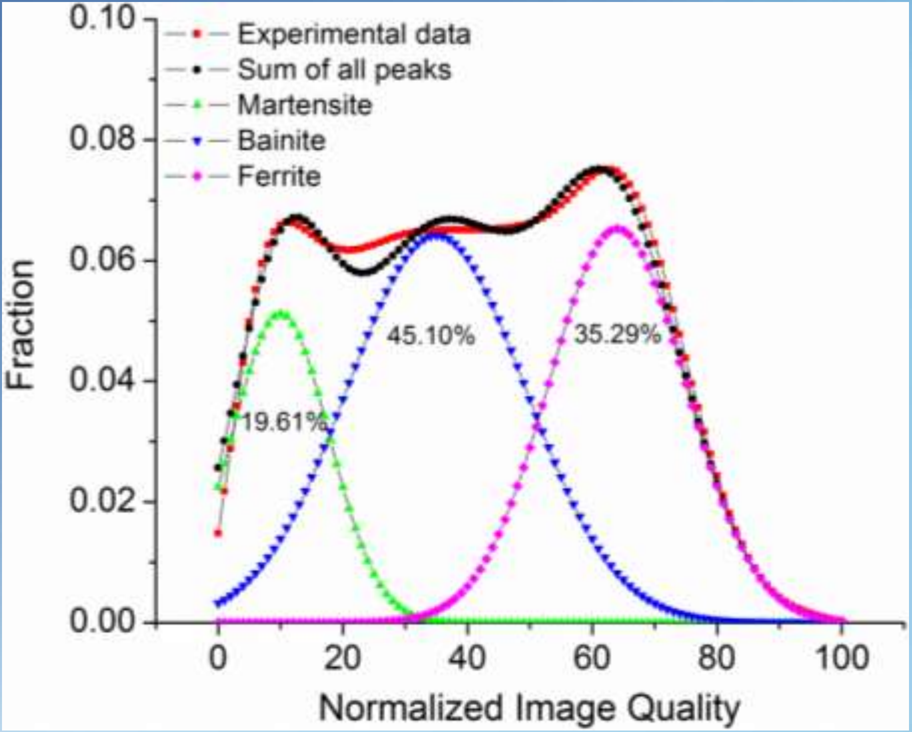

Mechanical properties resulting from Cycle A

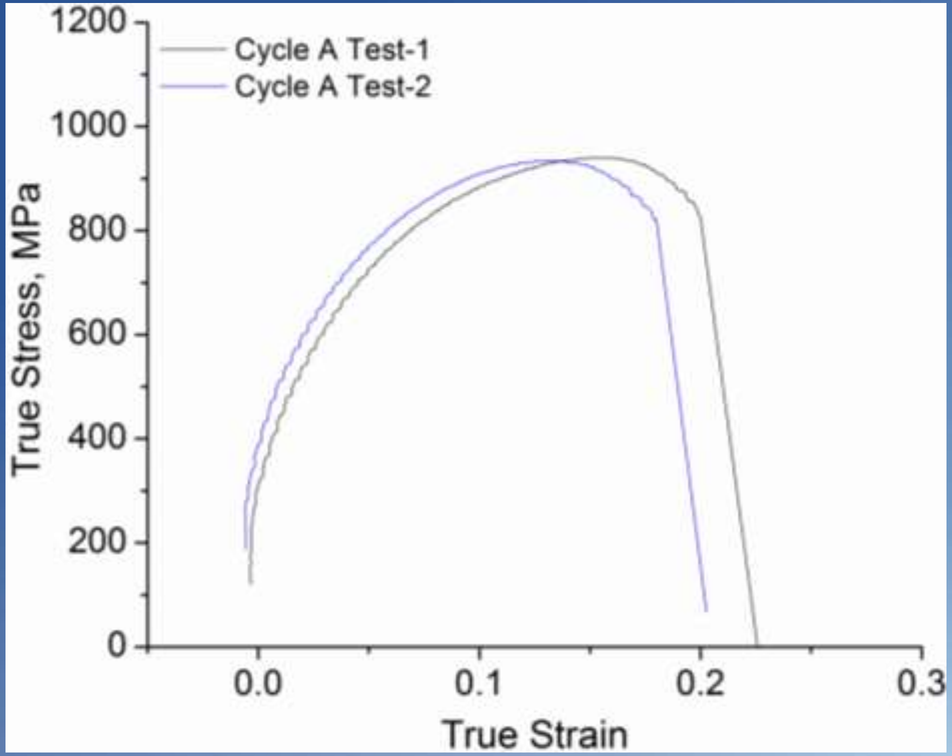

YS (MPa)	UTS (MPa)	EL (%)	*HR 15-N*
649 ± 3.53	962.3 ± 3.21	12.6 ± 1.15	

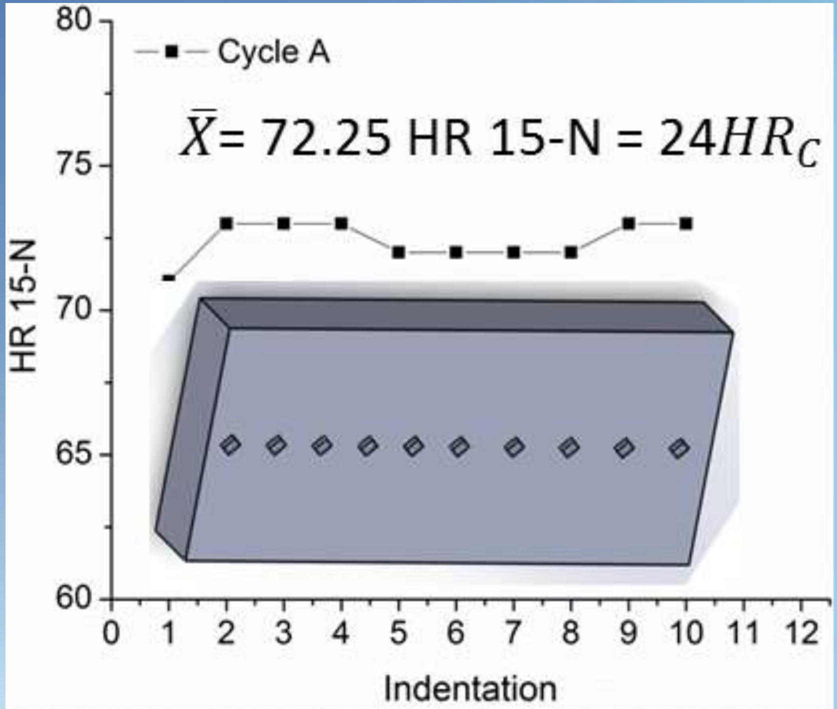

Fractography

SEM fractographs for the specimens tensile tested under thermal Cycle A condition.

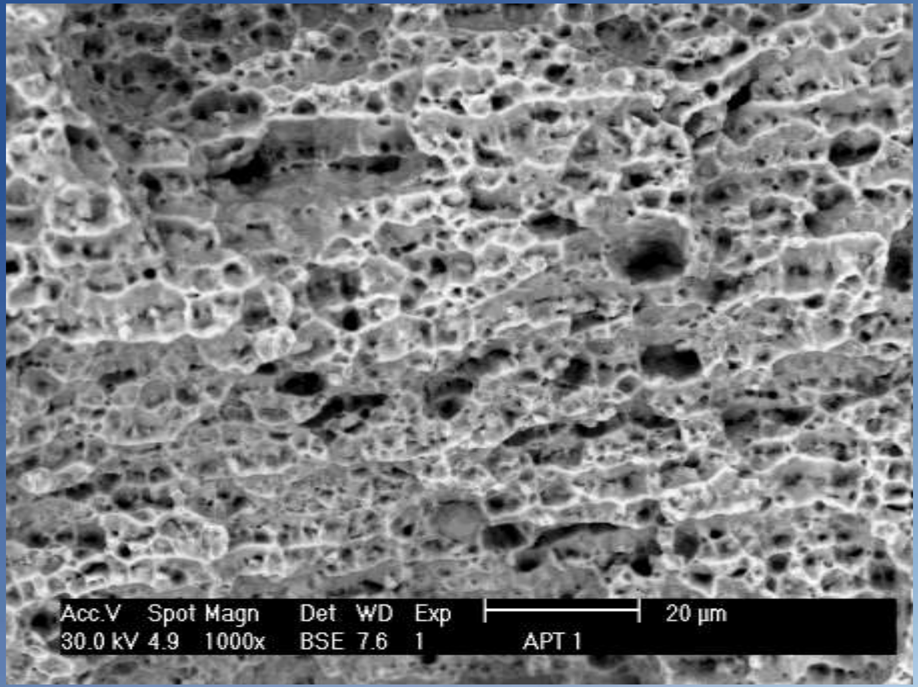

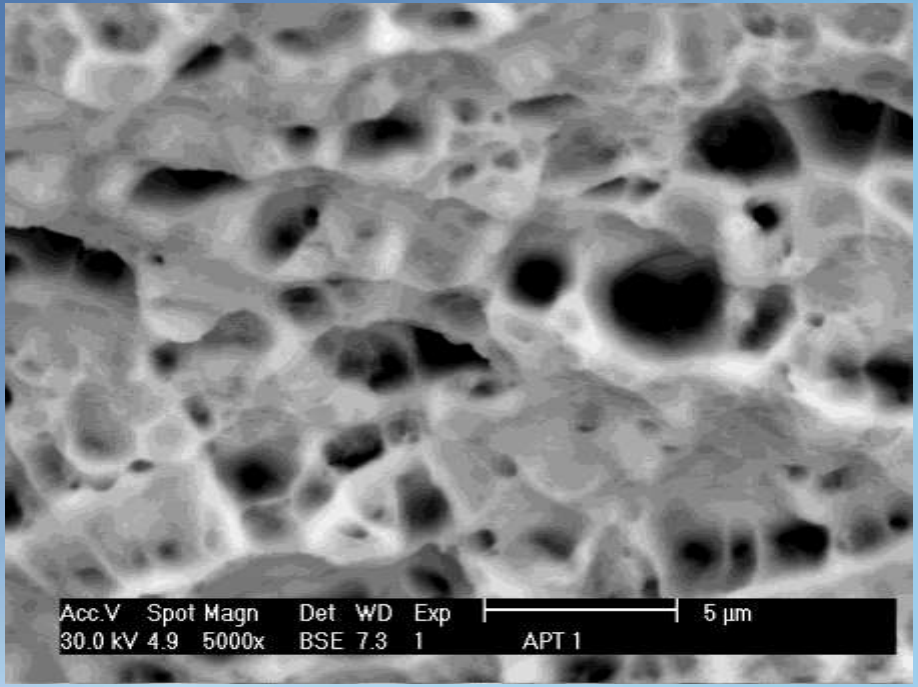

Microstructure and mechanical properties for additional cooling rates.

Thermal cycle and corresponding dilatometric curve resulting from the simulation of Cycle A for cooling rates of 1 and 100 °C/s.

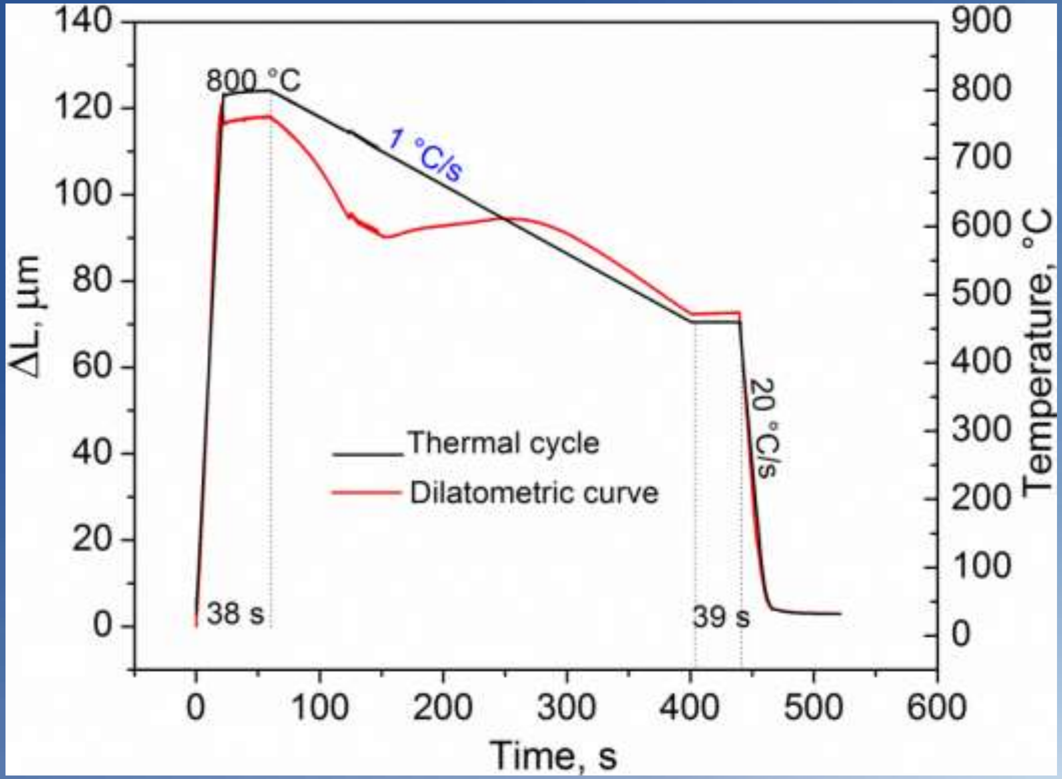

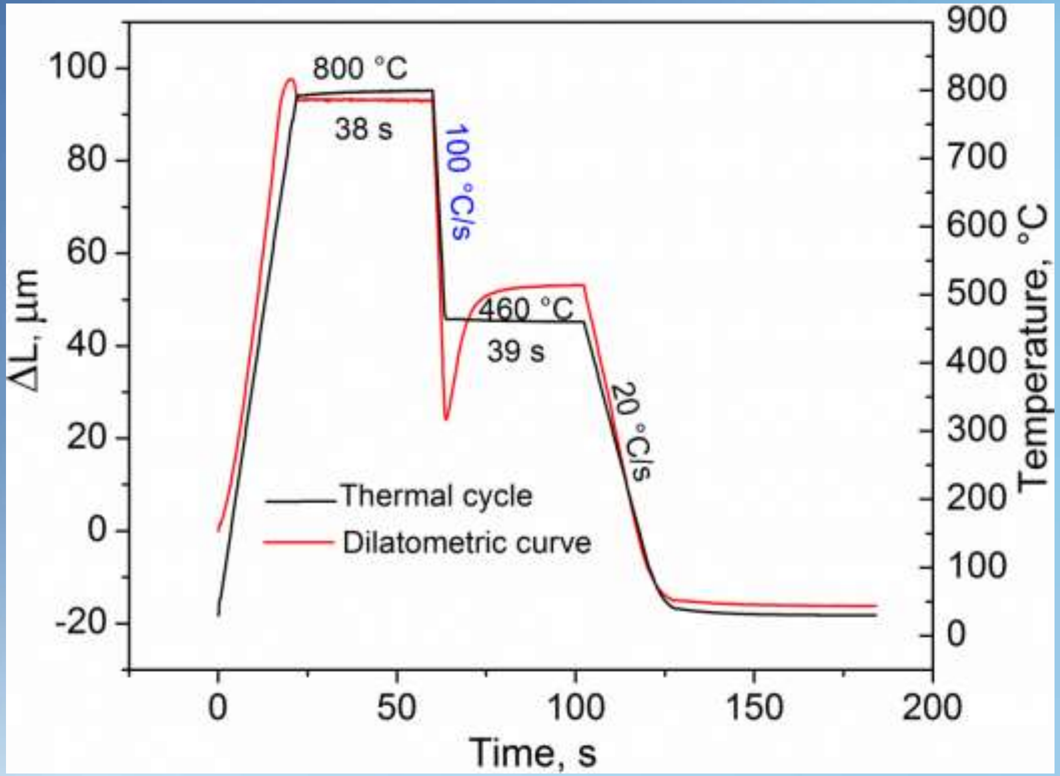

JMatPro calculation of linear expansion behavior as a function of temperature according to Cycle A and cooling rates of 1 and 100 °C/s.

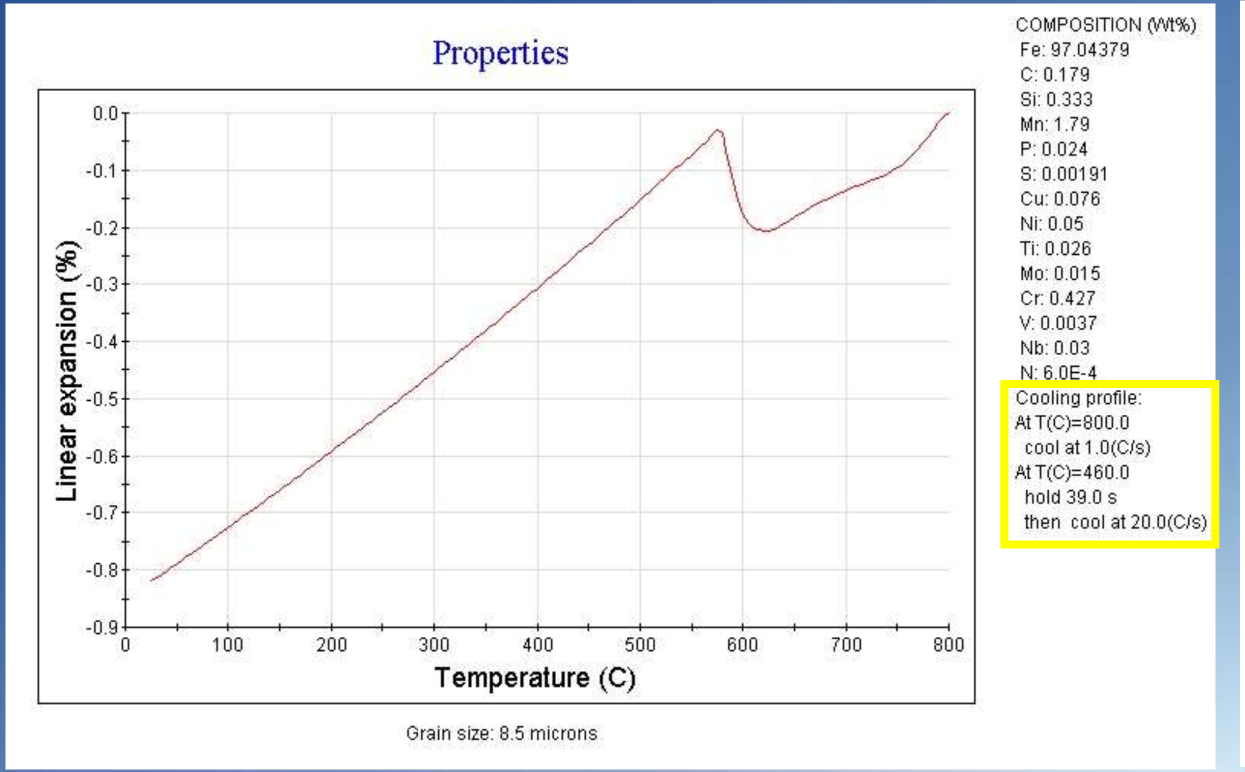

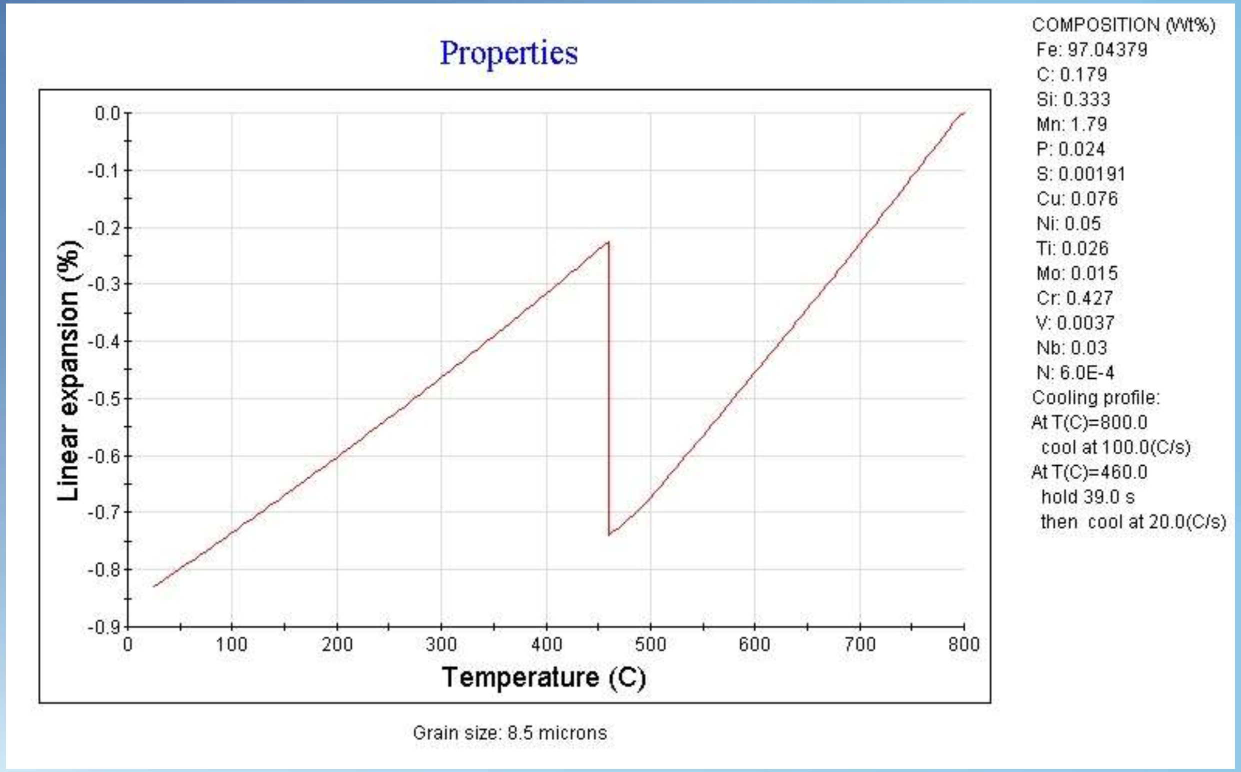

Prediction of resulting phases according to the cycle A and varying the cooling rate at 1 and 100 °C/s. For these heat treatmentes, the resulting microstructures would consist of (F+P) and (F+B+M), respectively.

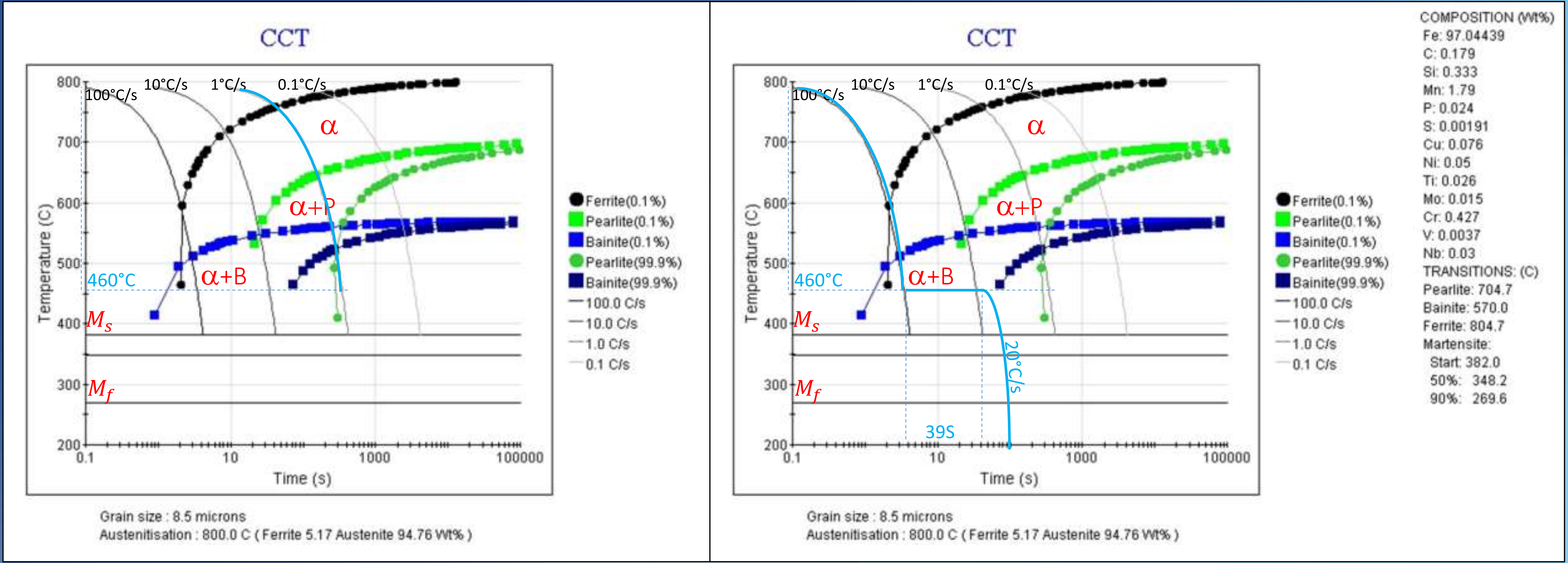

Temperature evolution of the volume fractions of individual phases for Cycle A and varying the cooling rate at 1 and 100 °C/s. According to *JmatPro* software, the transformed volume fractions would be (60% pearlite and 40% ferrite) and (90% bainite and 10% ferrite), respectively.

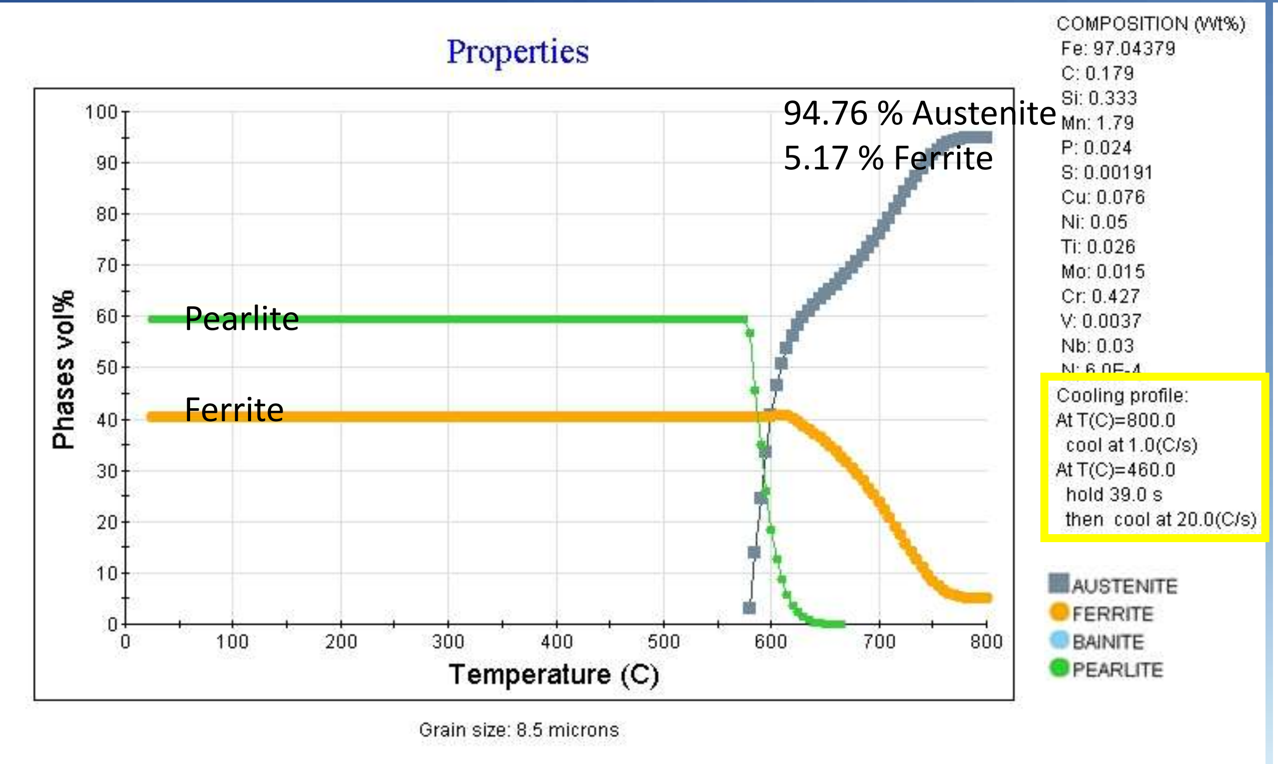

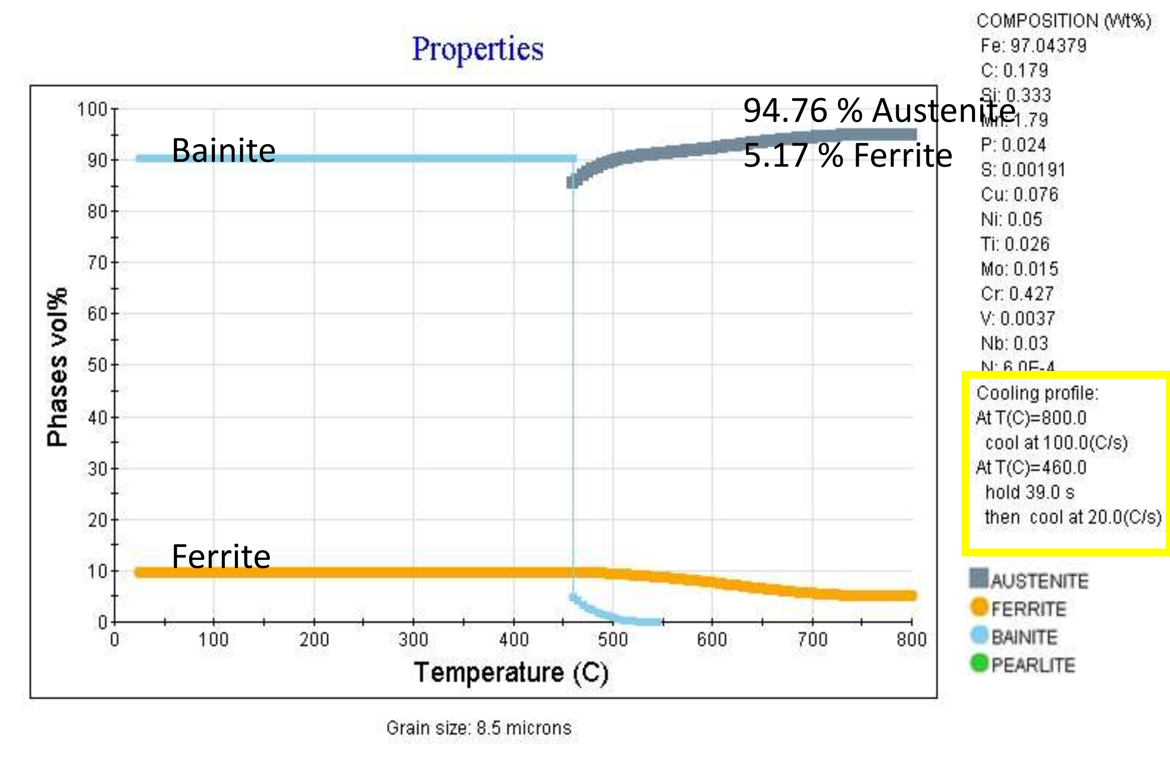

Microstructures and mechanical properties resulting of sample subjected to Cycle A varying the cooling rate at 1°C/s . Microstructures revealed by Nital 2%.

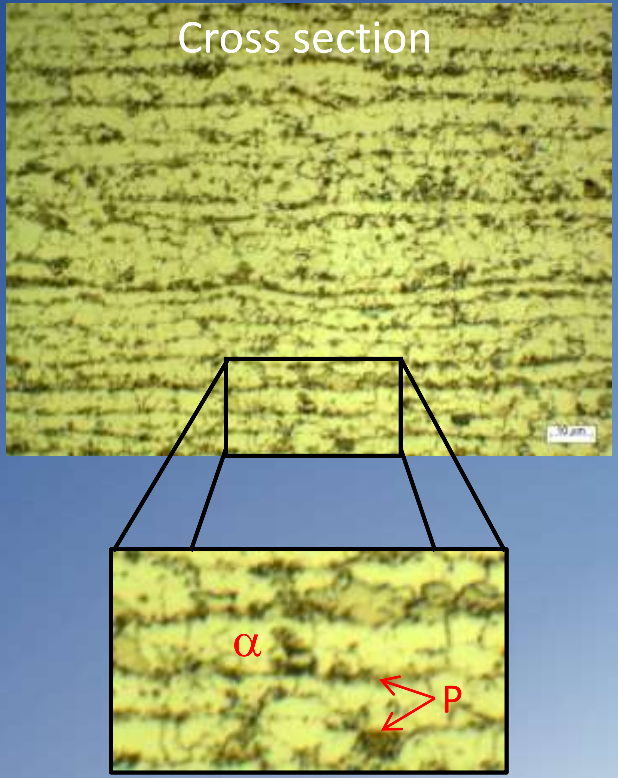

YS (MPa)	UTS (MPa)	EL (%)	*HR 15-N*
478	772 ± 8.48	13.8 ± 8.48	67.4 ± 3.35

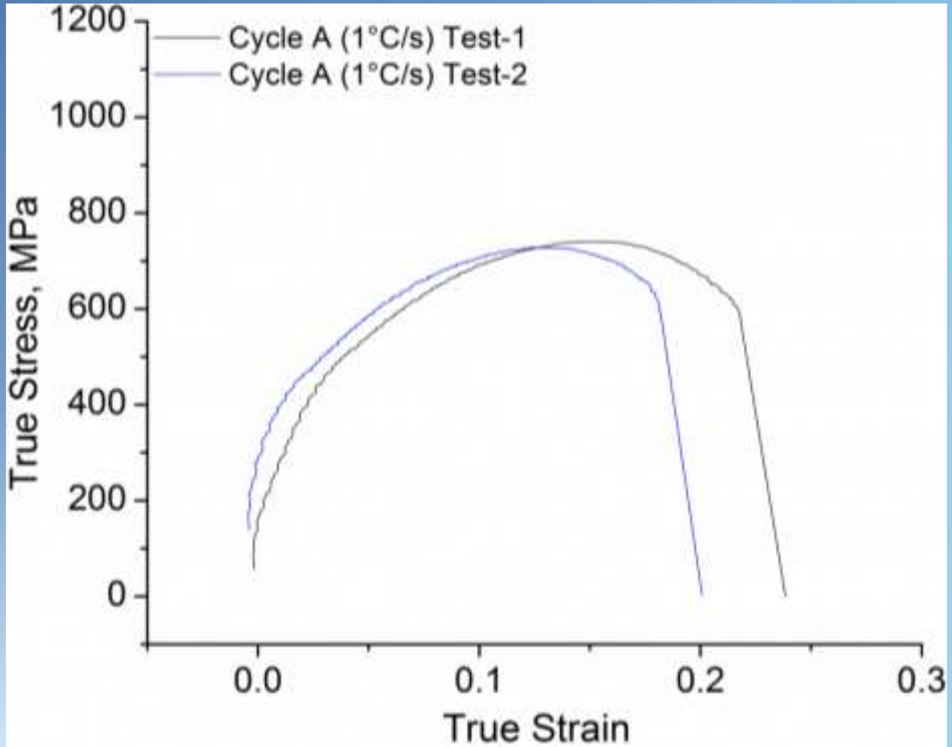

Microstructures and mechanical properties resulting of sample subjected to Cycle A varying the cooling rate at 100°C/s . Microstructures revealed by Nital 2%.

YS (MPa)	UTS (MPa)	EL (%)	*HR 15-N*
710	970 ± 9.19	11.2 ± 7.07	74.33 ± 0.81

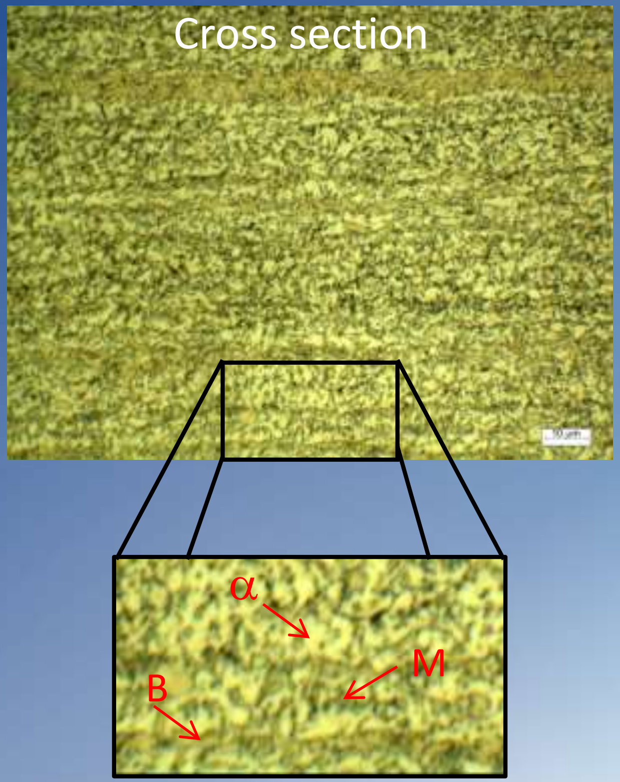

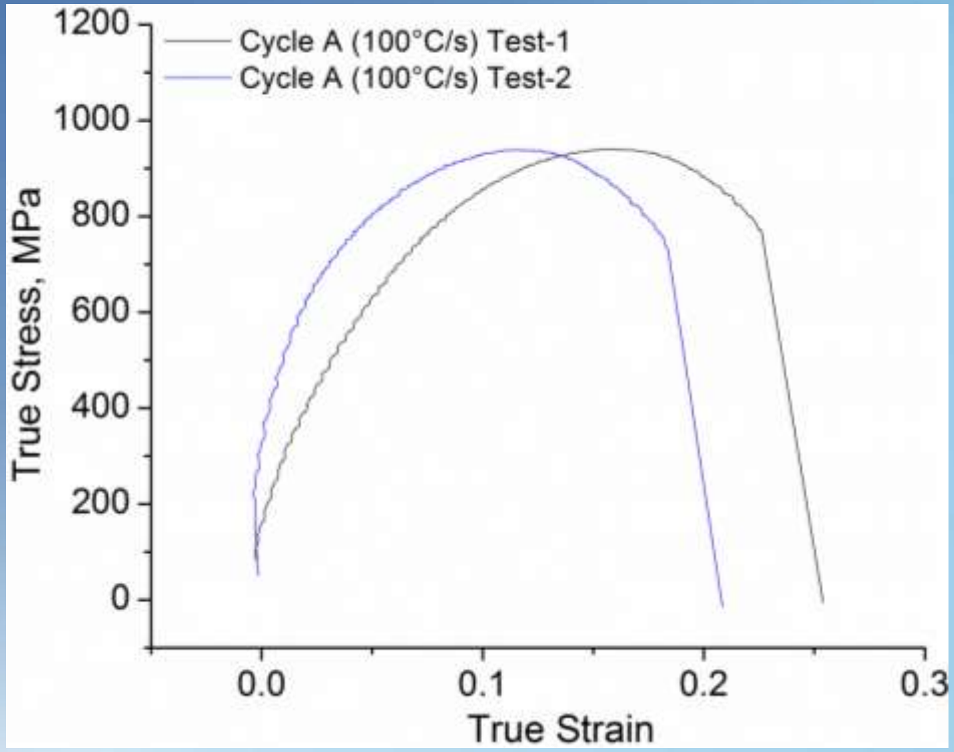

Simulation of thermal cycle B

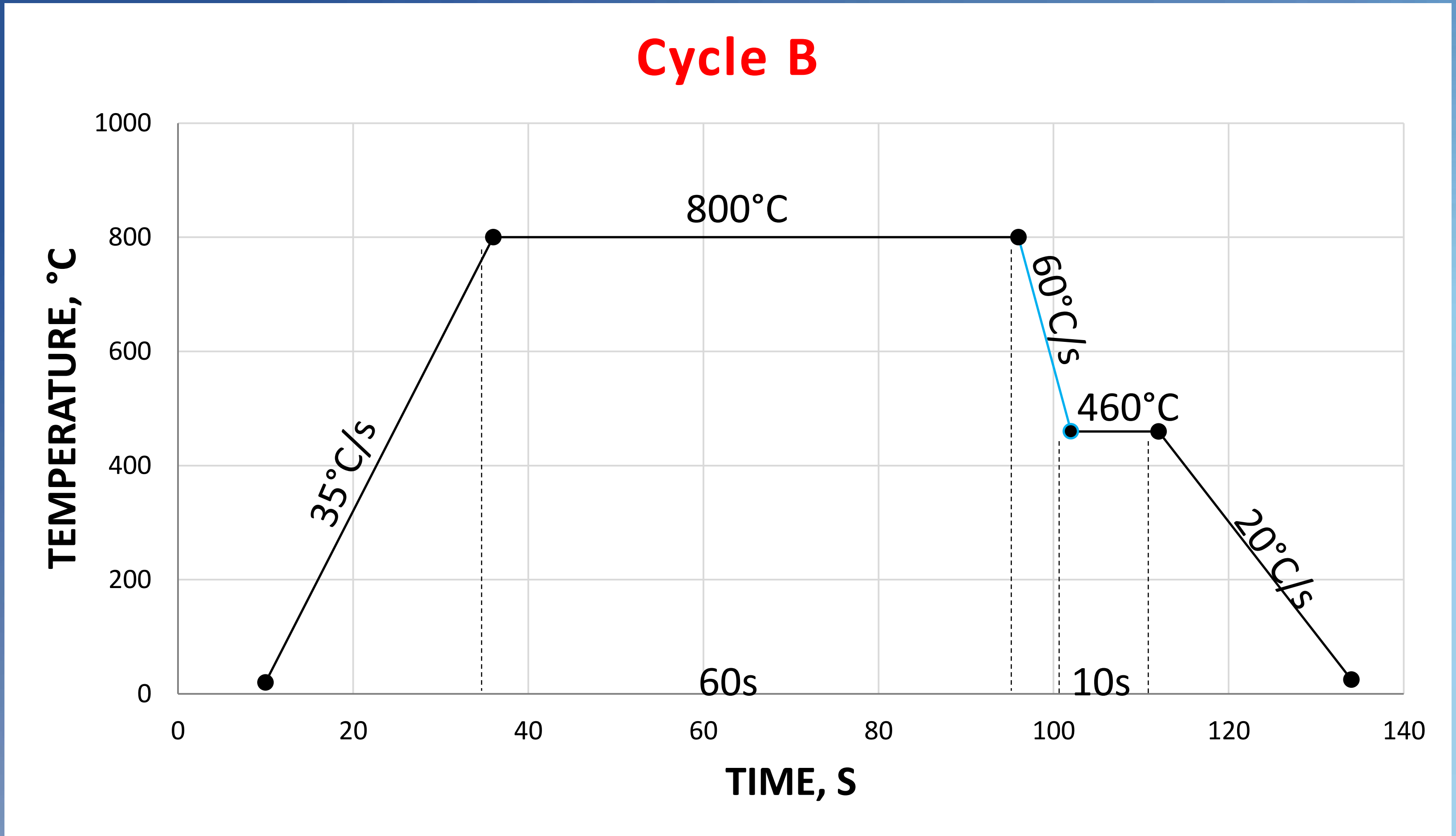

Metallographic characterization and hardness

Microstructures (optical and SEM micrographs) and hardness profile resulting of sample subjected to Cycle B. Microstructures revealed by 2% nital reagent.

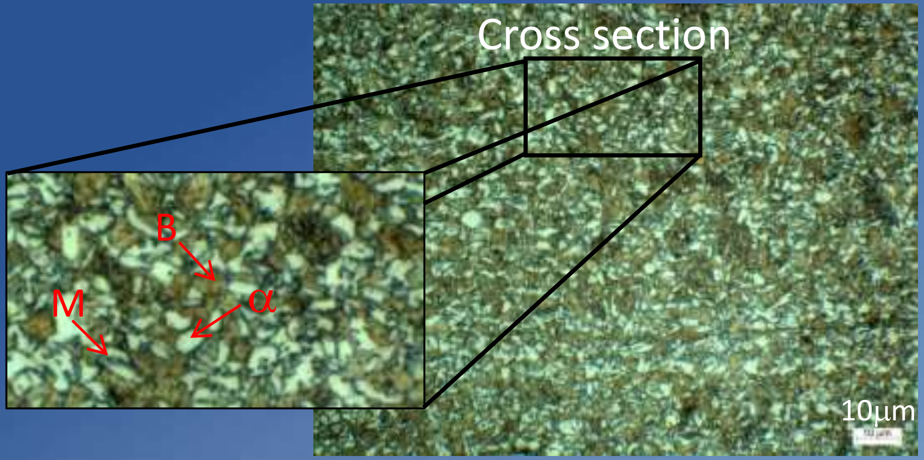

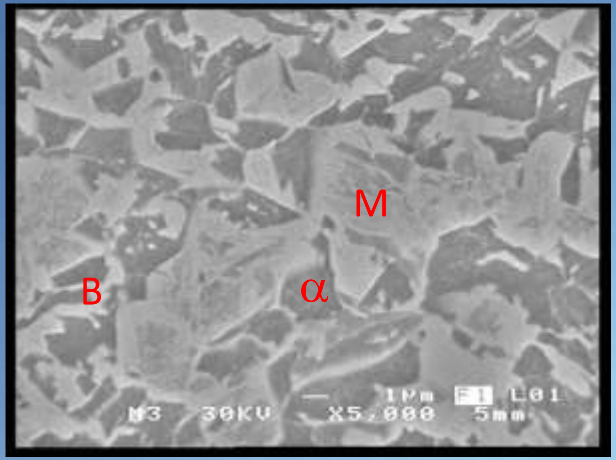

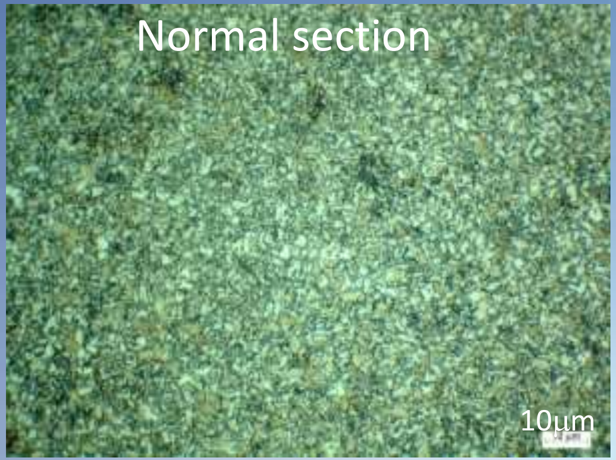

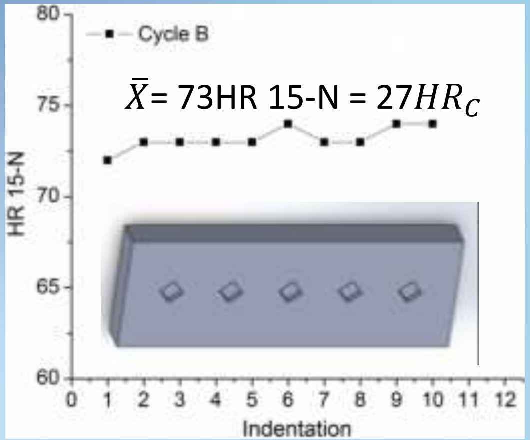

Microstructures (optical and SEM micrographs) resulting from sample subjected to Cycle B. The heat treated samples were etched with LePera.

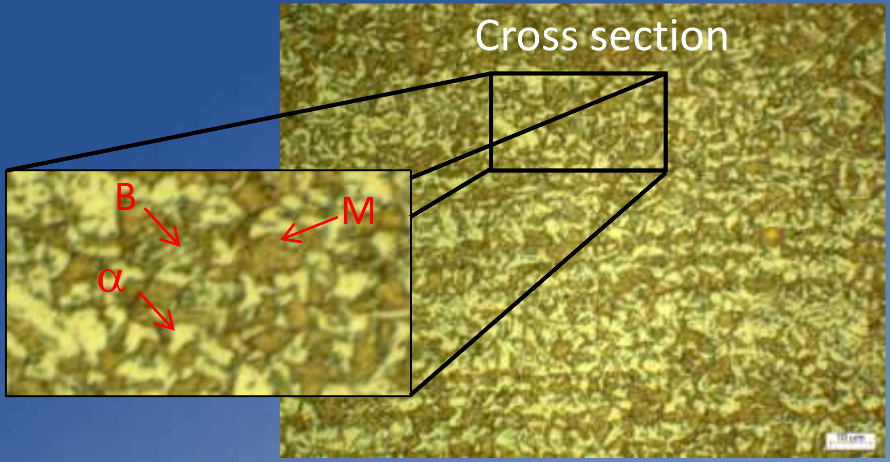

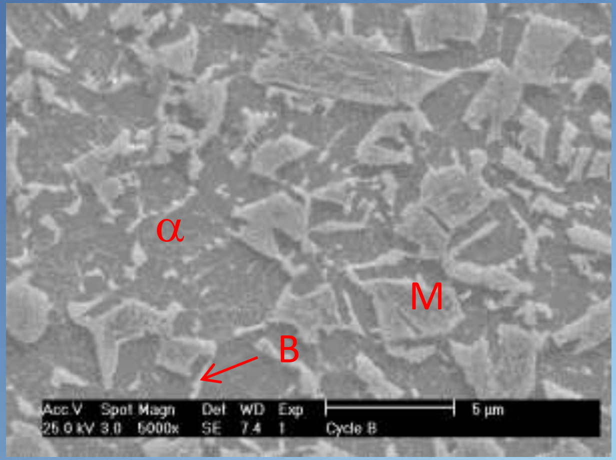

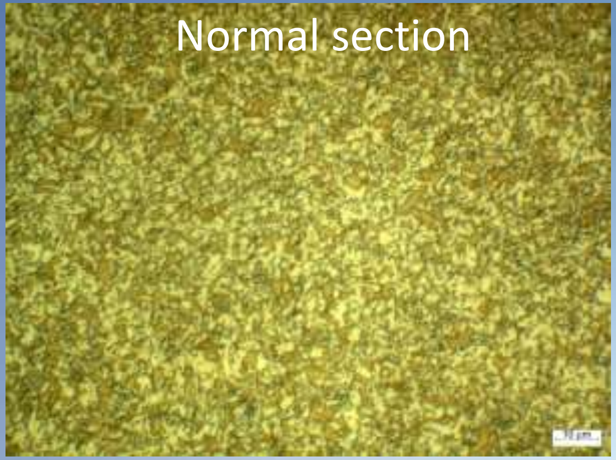

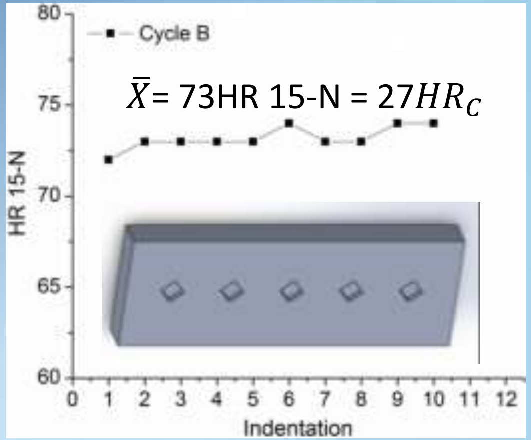

Microstructural characterization by OIM/EBSD

According to the processing of image quality values (IQ), the resulting phases from Cycle B are 35.19% martensite, 38.89% bainite and 25.93% ferrite.

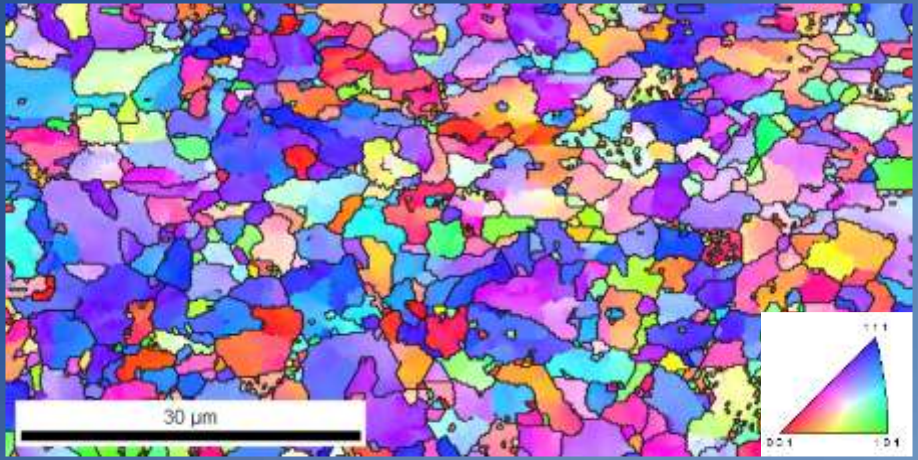

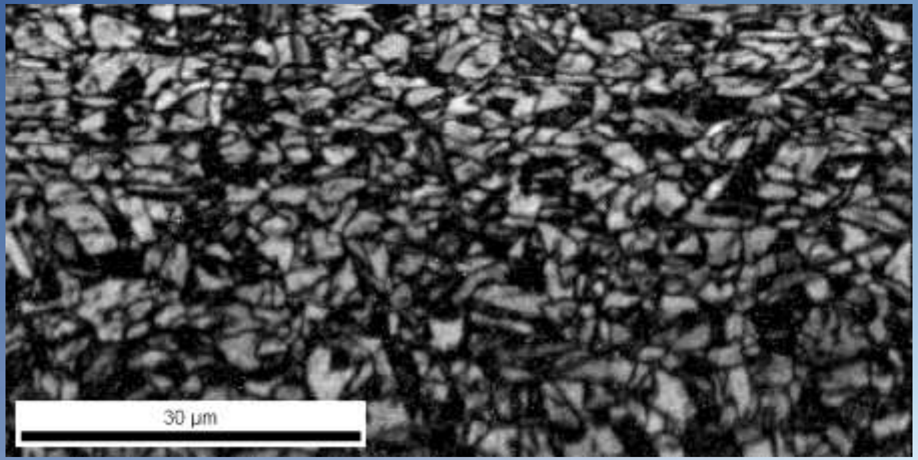

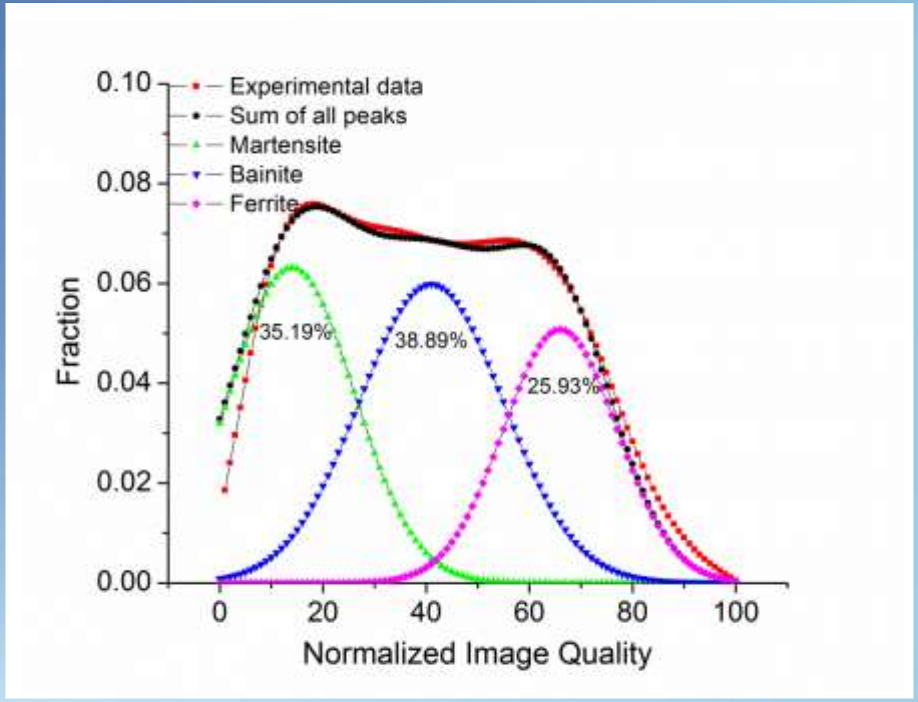

Mechanical properties resulting from Cycle B

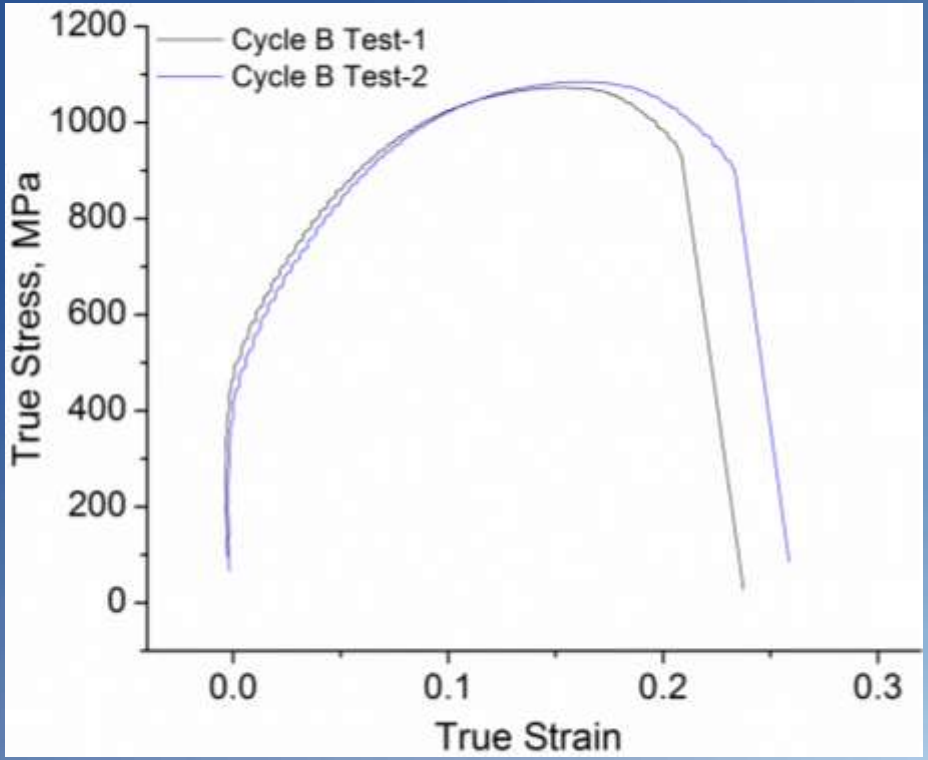

YS (MPa)	UTS (MPa)	EL (%)	*HR 15-N*
686 ± 6.36	1099 ± 7.77	16 ± 0.9	

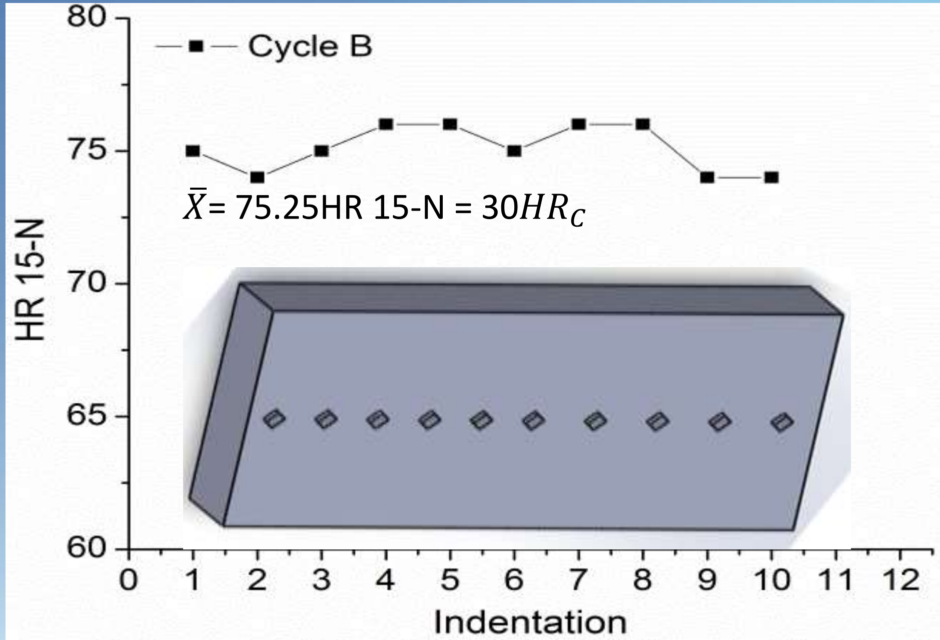

Fractography

SEM fractographs for the specimens tensile tested under thermal Cycle B condition.

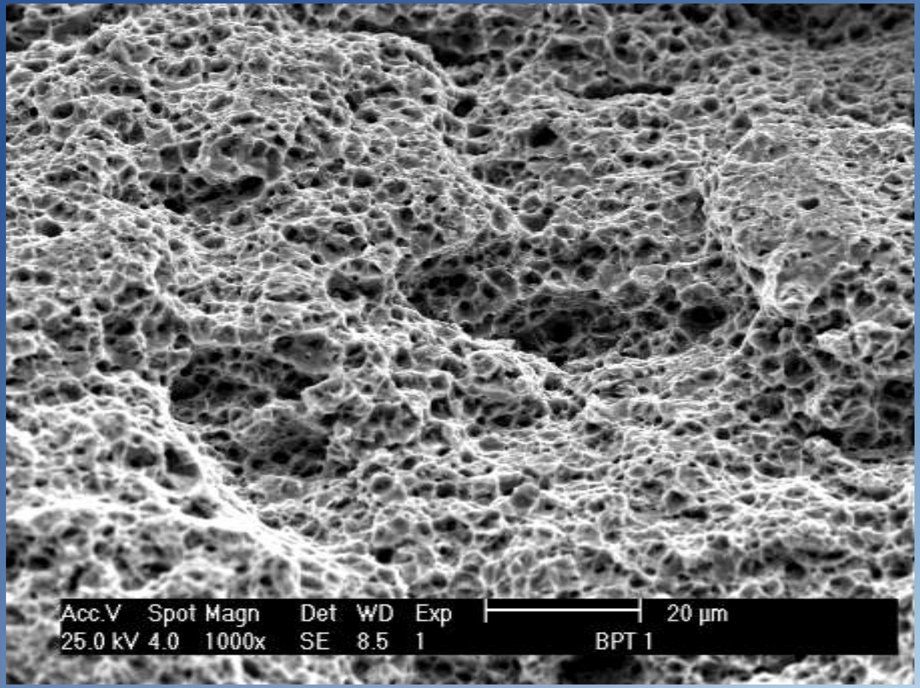

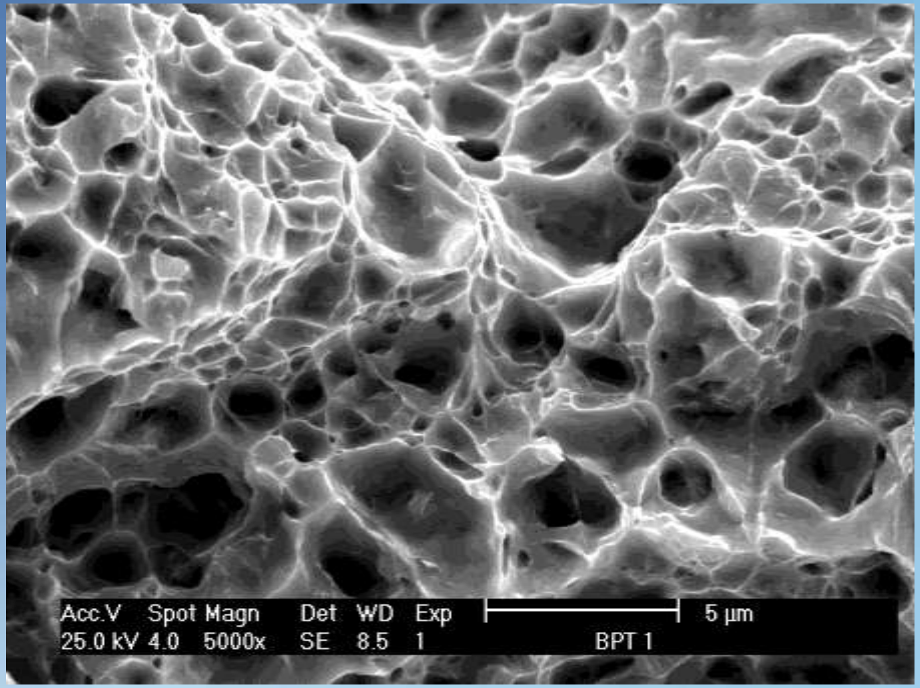

Thermal cycle and corresponding dilatometric curve resulting from the simulation of Cycle B for cooling rates of 1 and 100 °C/s.

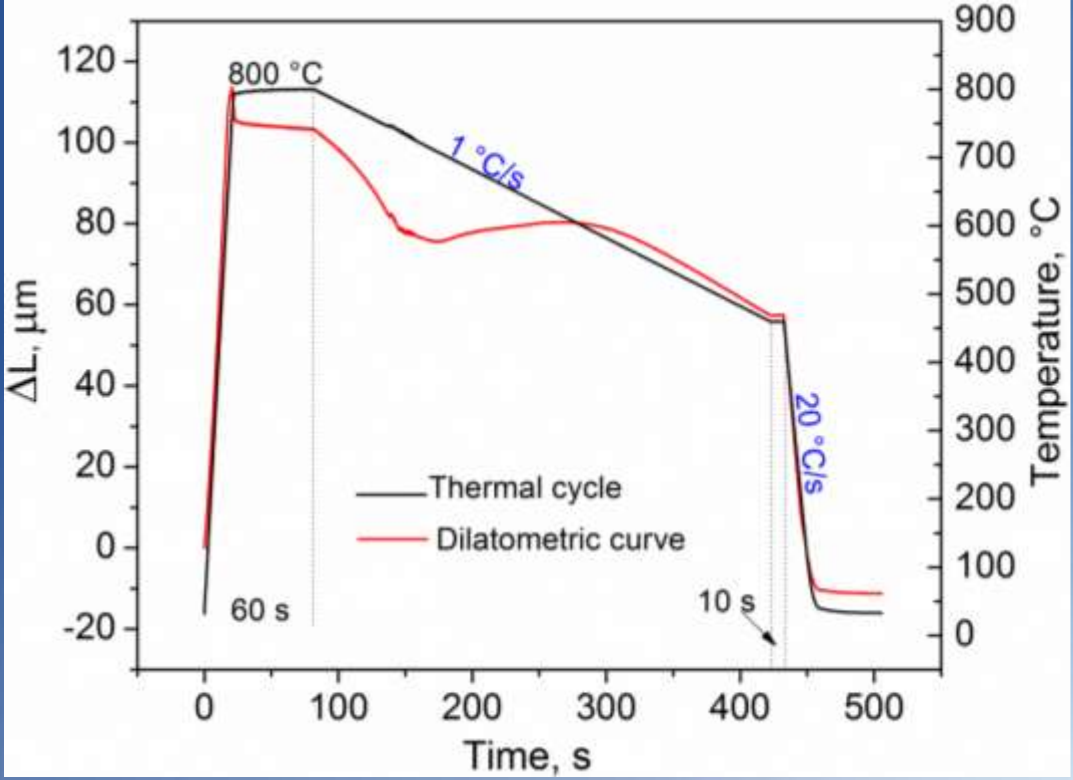

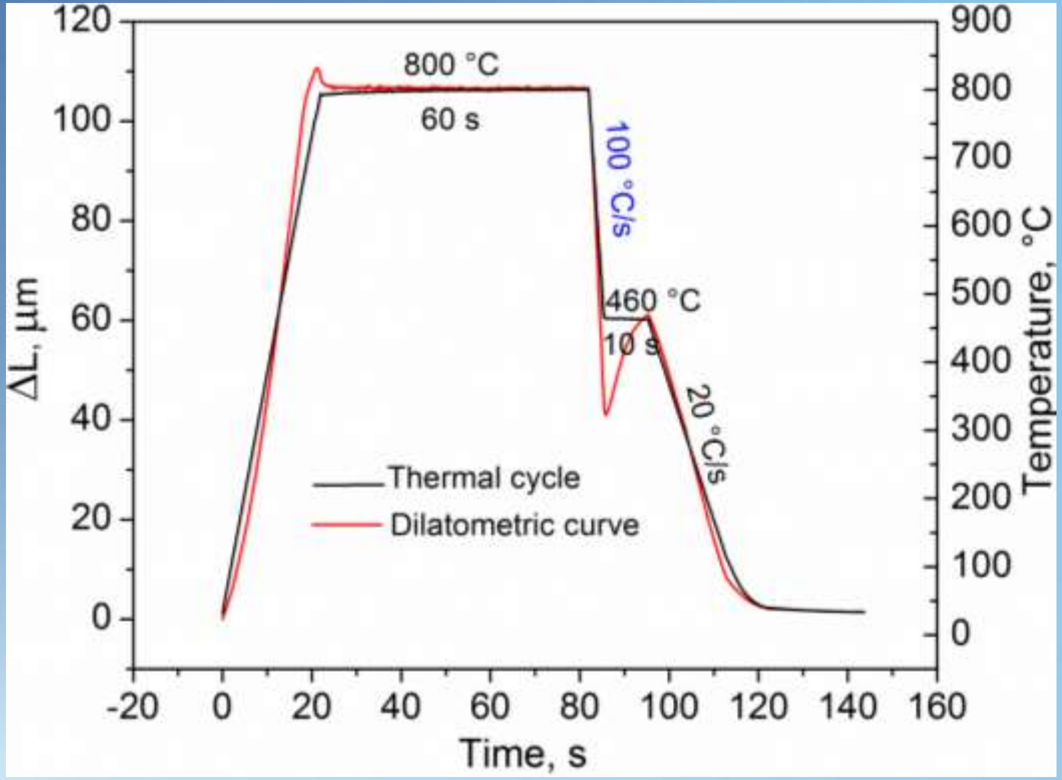

JMatPro calculation of linear expansion behavior as a function of temperature according to Cycle B and cooling rates of 1 and 100 °C/s.

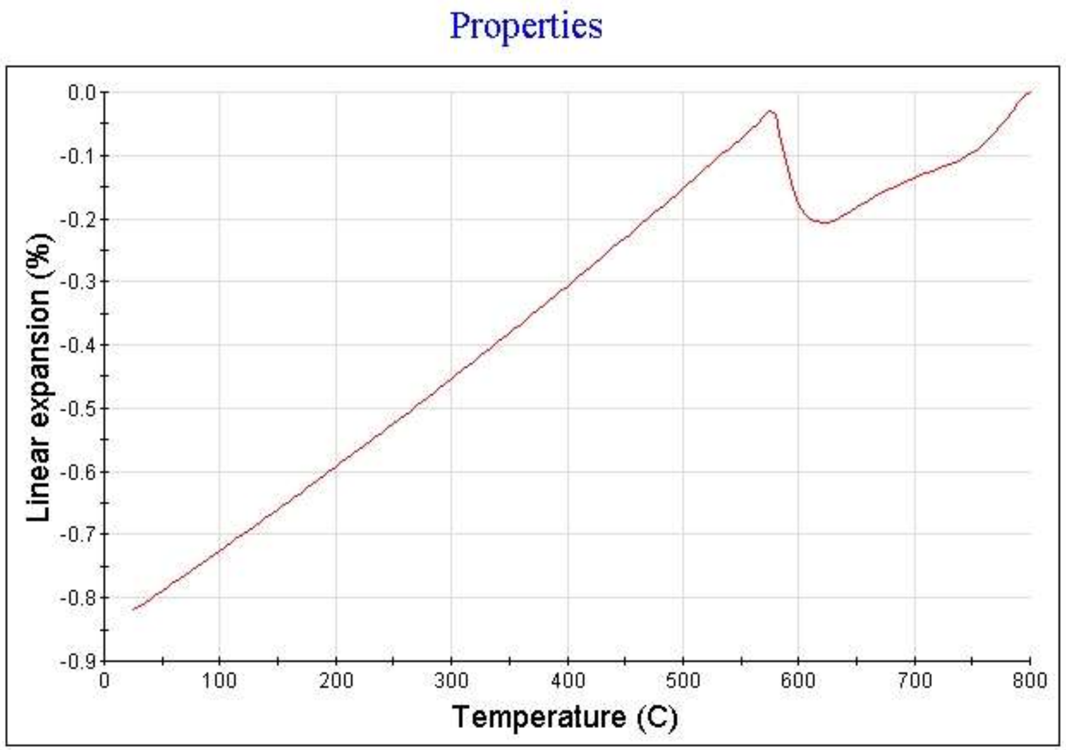

Grain size: 8.5 microns

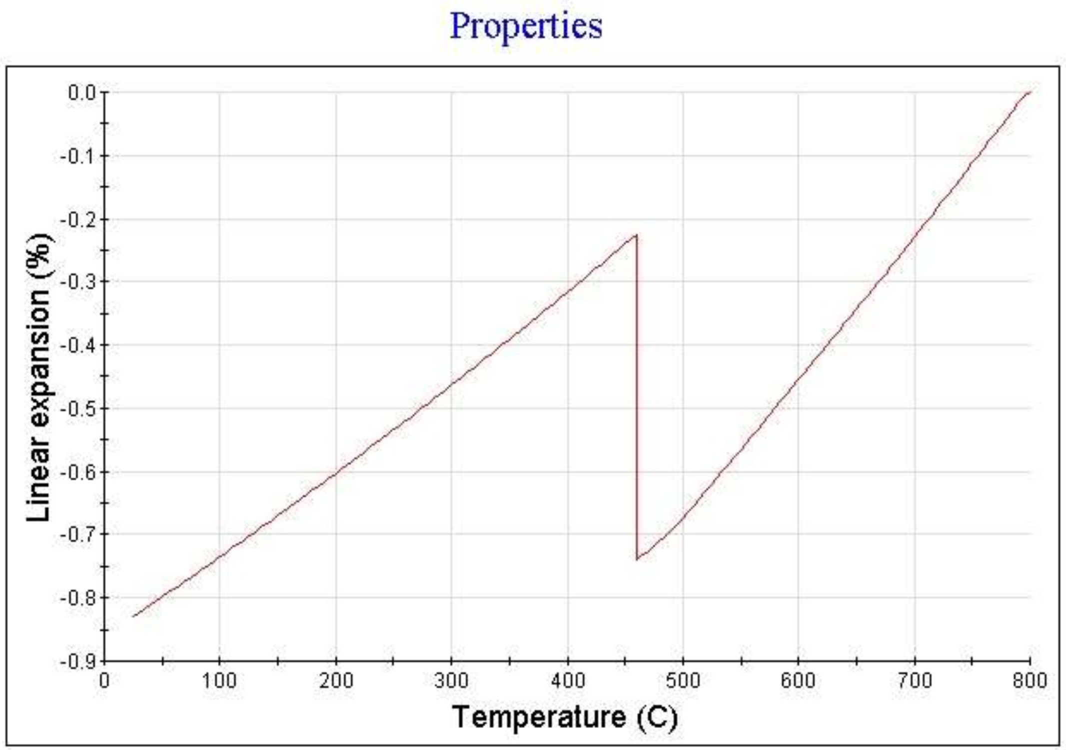

Grain size: 8.5 microns

COMPOSITION (Wt%)
Fe: 97.04379
C: 0.179
Si: 0.333
Mn: 1.79
P: 0.024
S: 0.00191
Cu: 0.076
Ni: 0.05
Ti: 0.026
Mo: 0.015
Cr: 0.427
V: 0.0037
Nb: 0.03
N: 6.0E-4
Cooling profile:
At T(C)=800.0
cool at 100.0(C/s)
At T(C)=460.0
hold 10.0 s
then cool at 20.0(C/s)

Prediction of resulting phases according to the cycle B and varying the cooling rate at 1 and 100 °C/s. For these heat treatmentes, the resulting microstructures would consist of (F+P) and (F+B+M), respectively.

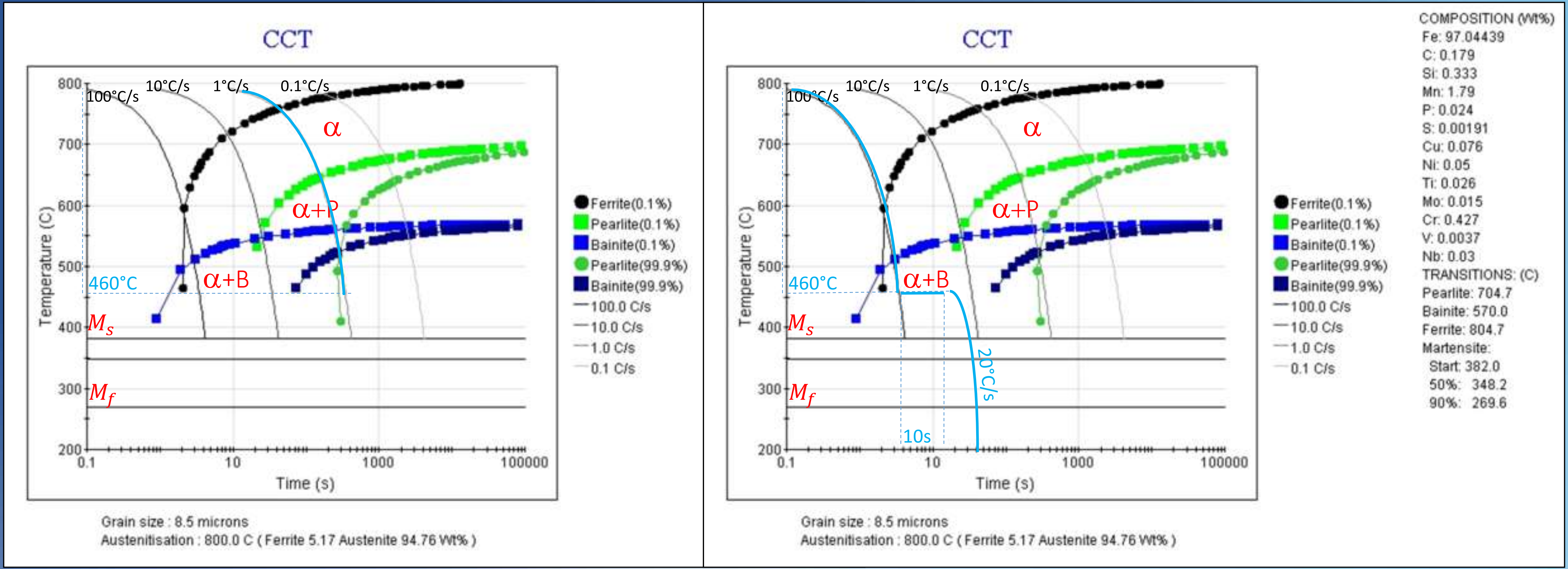

Temperature evolution of the volume fractions of individual phases for Cycle B and varying the cooling rate at 1 and 100 °C/s. According to *JmatPro* software, the transformed volume fractions would be (60% pearlite and 40% ferrite) and (90% bainite and 10% ferrite), respectively.

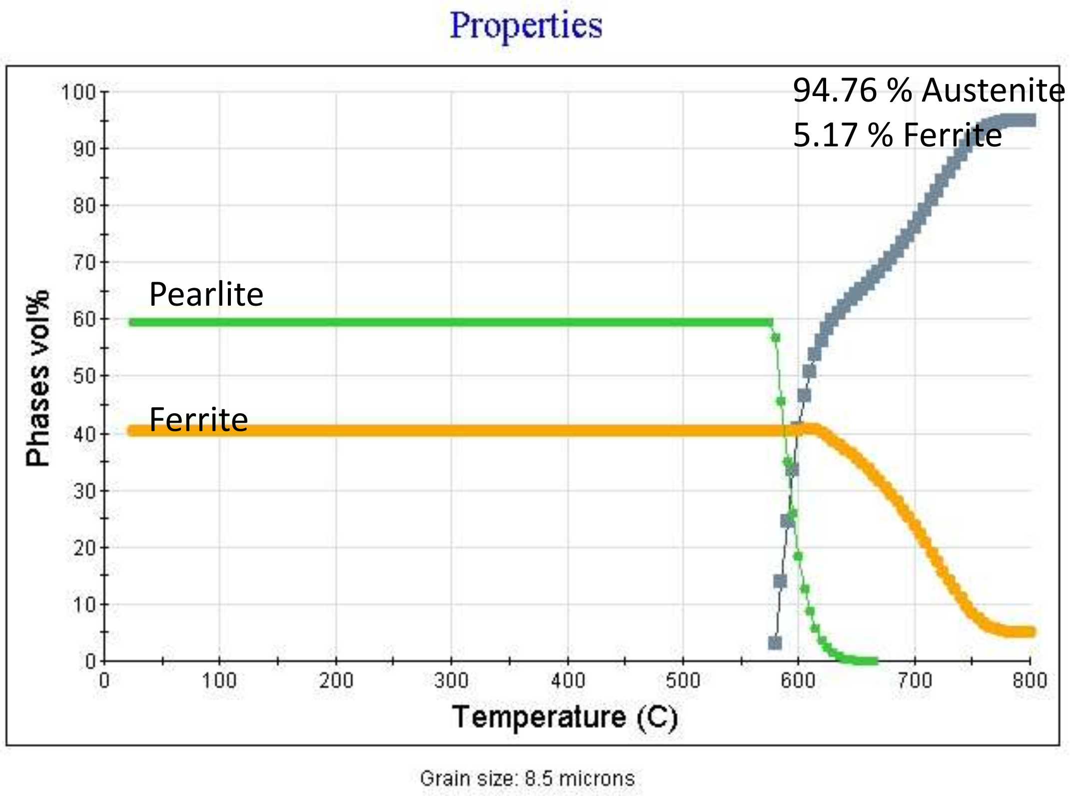

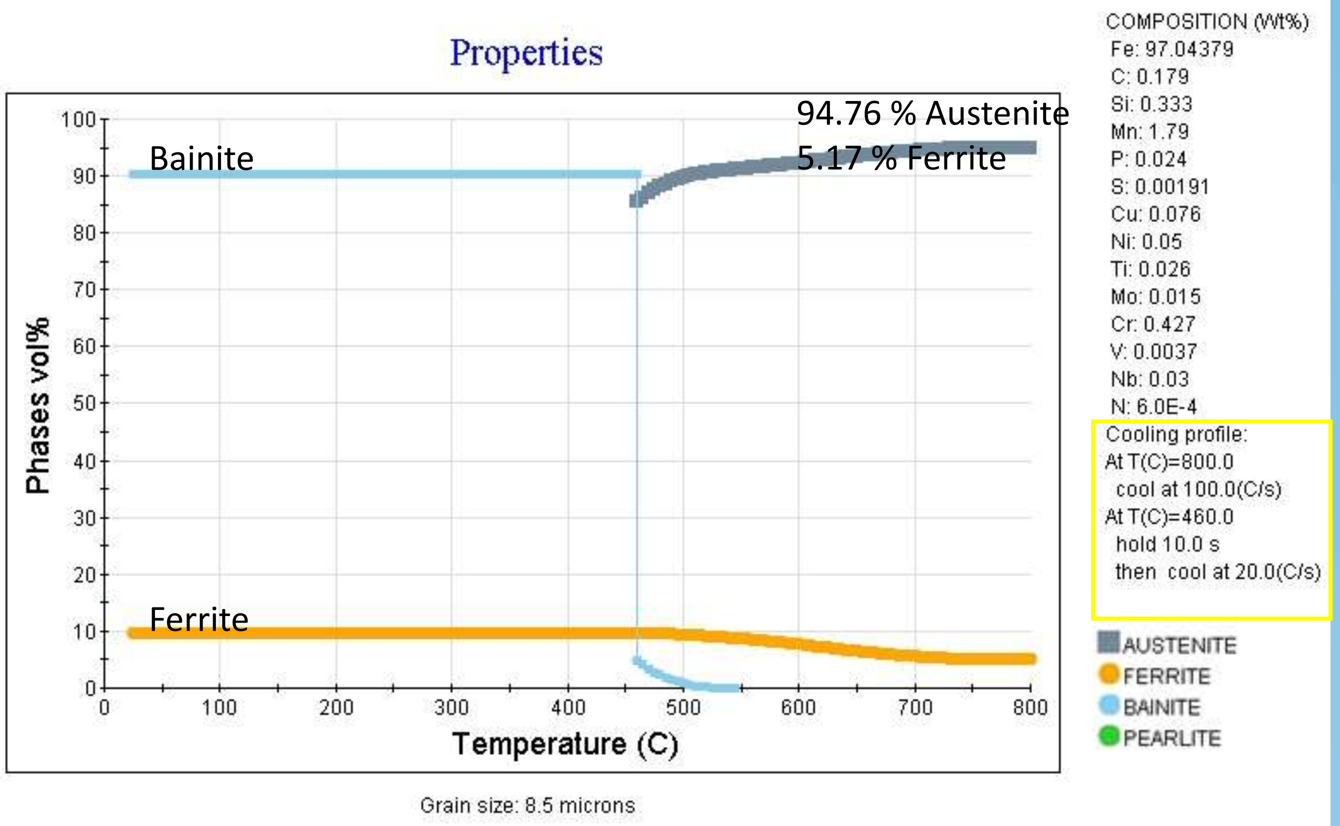

Microstructures and mechanical properties resulting of sample subjected to Cycle B at a cooling rate at 1°C/s . Microstructures revealed by Nital 2%.

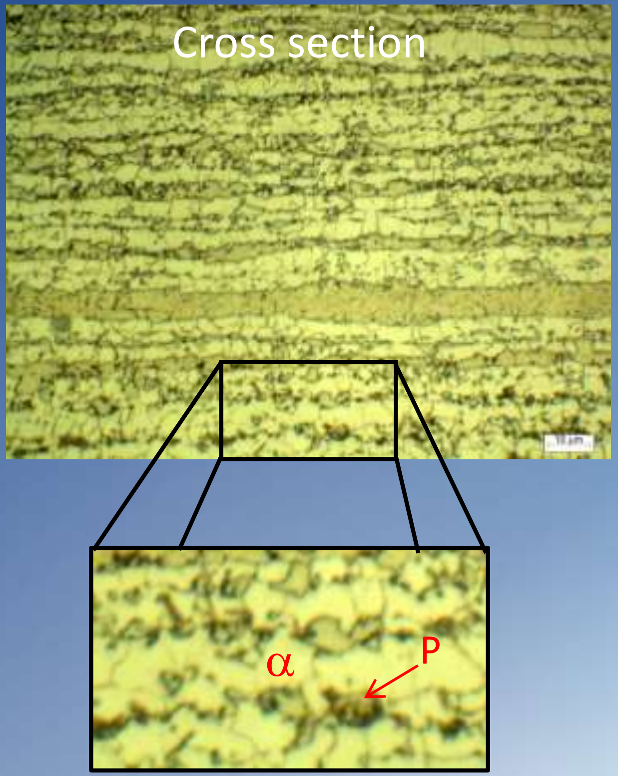

YS (MPa)	UTS (MPa)	EL (%)	*HR 15-N*
517	773 ± 7.77	14.7 ± 2.12	69 ± 1.73

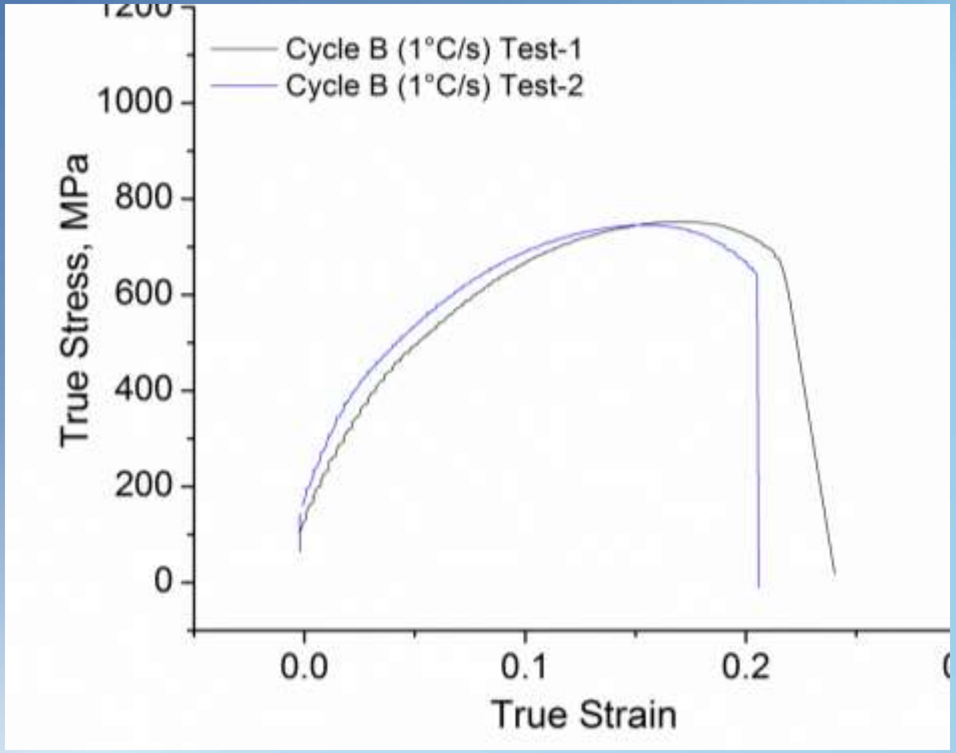

Microstructures and mechanical properties resulting of sample subjected to Cycle B varying the cooling rate at 100°C/s . Microstructures revealed by Nital 2%.

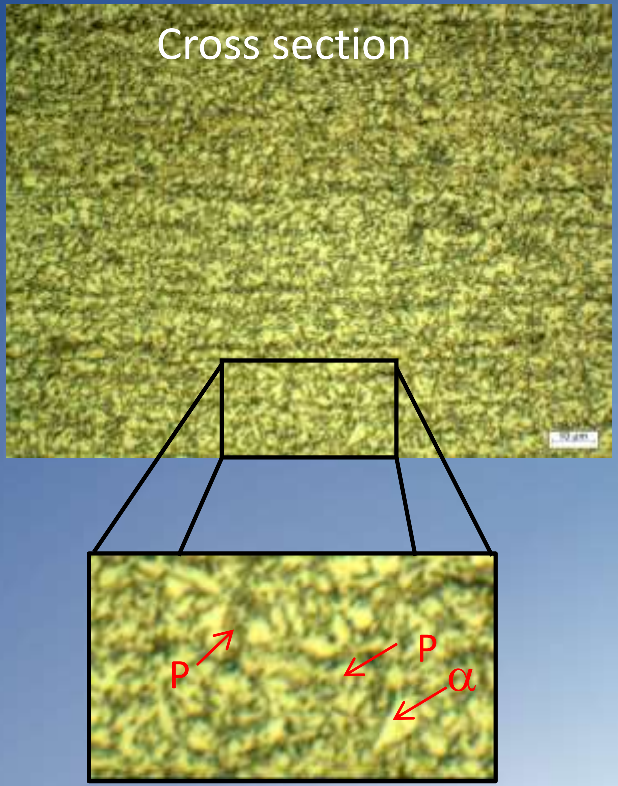

YS (MPa)	UTS (MPa)	EL (%)	*HR 15-N*
721	1078 ± 9.89	10.5 ± 3	73.2 ± 0.44

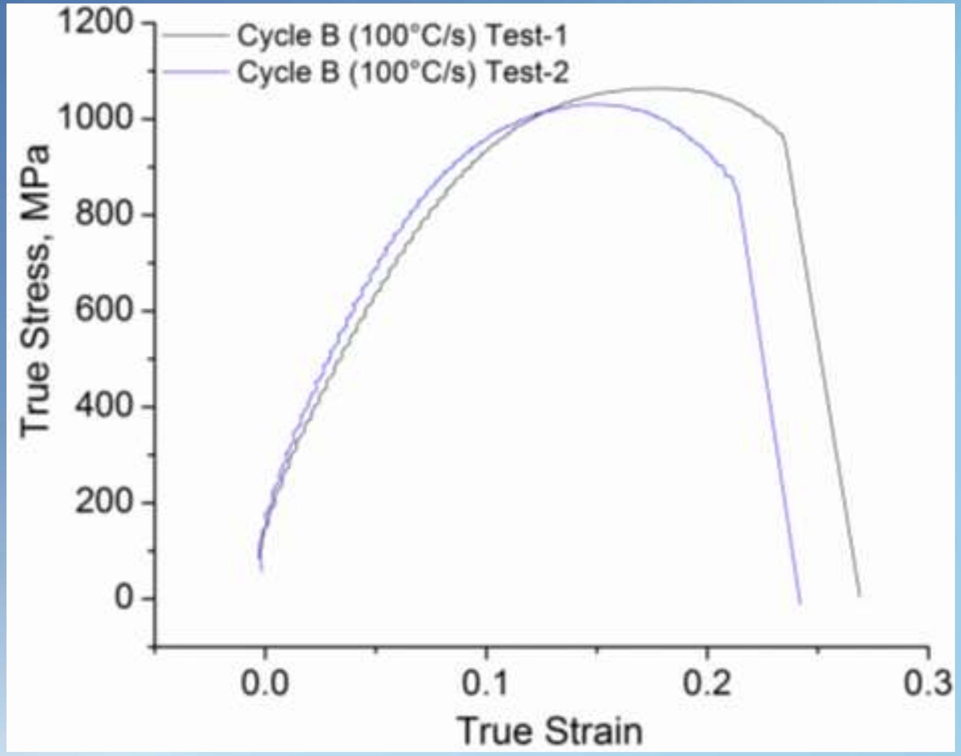

Conclusions

<u>Actual customer target</u>:

YS (MPa)	UTS (MPa)	EL (%)
550 - 730	> 980	> 8

Thermal cycle	% Phases		Mechanical properties		
	JMatPro	EBSD	YS (MPa)	UTS (MPa)	EL (%)
Cycle A	78% bainite, 22% ferrite	19.61% martensite, 45.10% bainite, 35.29% ferrite	649 ± 3.53	962 ± 3.21	12.6 ± 1.15
Cycle B	88% bainite, 12%ferrite	35.19% martensite, 38.89% bainite, 25.93% ferrite	686 ± 6.36	1099 ± 7.77	16.0 ± 0.9
Cycle B with overaing	50% bainite, 38% martensite, 12% ferrite	-	668 ± 4.9	1011 ± 4.93	11.4 ± 0.65

Figure 1. Evolution of TS and Ys with martenste fractin for the Fe-Mn-C steels (*Davies R.G. Influence of martensite composition and content on the properties of dual phase steels, Met Trans. A. vol 9A. 1978. Pp 671-679*)

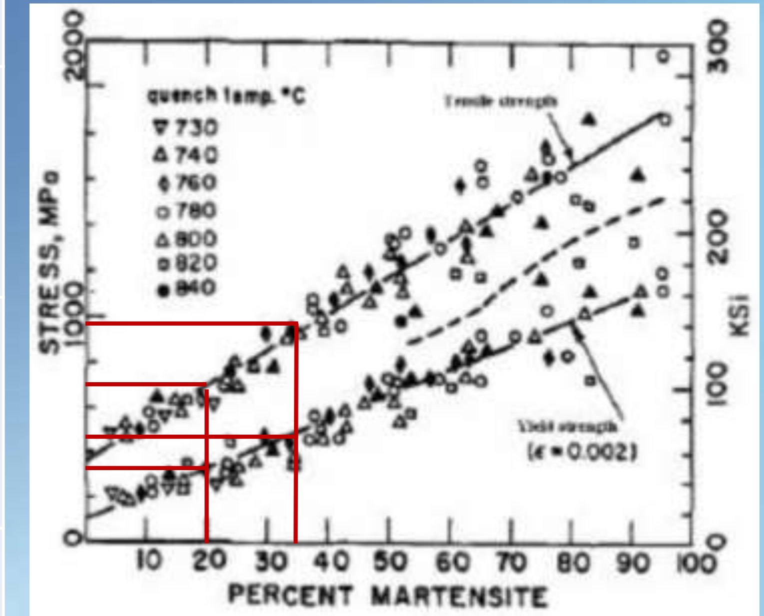

Conclusions

Actual customer target:

YS (MPa)	UTS (MPa)	EL (%)
550 - 730	> 980	> 8

Thermal cycle	Cooling rate (°C/s)	Mechanical properties		
		YS (MPa)	UTS (MPa)	EL (%)
Cycle A	1	478 ± 8.48	772 ± 8.48	13.8 ± 0.25
	100	710 ± 7.07	970 ± 9.19	11.2 ± 0.15
Cycle B	1	517 ± 2.12	773 ± 7.77	14.7 ± 0.07
	100	721 ± 3	1078 ± 9.89	10.5 ± 0.25

Conclusions

- The use of *JMatPro* commercial software allows to predict the transformation behavior of cold rolled DP1000 steel. However, it does not predict solute segregation to austenite during isothermal holding.
- Thermal Cycle B produces the required mechanical properties.
- Cooling rates between 10 and 100 °C/s produce multiphase microstructures consisting of ferrite, bainite and martensite. However, there is a limit for the mechanical properties that may be achieved.
- With the present results the first stage of this research project is concluded.